1 **Non-invasive stimulation of the human striatum disrupts reinforcement learning of**
2 **motor skills**

3

4 Pierre Vassiliadis[1,2,3], Elena Beanato[1,2], Traian Popa[1,2], Fabienne Windel[1,2], Takuya Morishita[1,2],
5 Esra Neufeld[4], Julie Duque[3], Gerard Derosiere[3,5], Maximilian J. Wessel[1,2,6] and Friedhelm C. Hummel[1,2,7] *

6

7

8 [1]Defitech Chair of Clinical Neuroengineering, Neuro-X Institute (INX) and Brain Mind Institute (BMI), École
9 Polytechnique Fédérale de Lausanne (EPFL), 1202 Geneva, Switzerland.

10 [2]Defitech Chair of Clinical Neuroengineering, INX and BMI, EPFL Valais, Clinique Romande de
11 Réadaptation,1951 Sion, Switzerland.

12 [3]Institute of Neuroscience, Université Catholique de Louvain, 1200, Brussels, Belgium

13 [4]Foundation for Research on Information Technologies in Society, Zurich, Switzerland

14 [5]Lyon Neuroscience Research Center – Impact team - Inserm U1028 – CNRS UMR5292, Lyon 1
15 University, Bron, France

16 [6]Department of Neurology, University Hospital, Julius-Maximilians-University, Würzburg, Germany

17 [7]Clinical Neuroscience, University of Geneva Medical School, 1202 Geneva, Switzerland.

18

19

20 *** CORRESPONDENCE TO:**

21 **Friedhelm C. Hummel**

22 Neuro-X Institute (INX)

23 École Polytechnique Fédérale de Lausanne (EPFL)

24 Campus Biotech, Room H4.3.132.084

25 Chemin des Mines 9, 1202 Geneva, Switzerland

26 and

27 EPFL Valais,

28 Clinique Romande de Réadaptation

29 Av. Grand-Champsec 90,

30 CH-1951 Sion

31 Email: friedhelm.hummel@epfl.ch

Abstract

Reinforcement feedback can improve motor learning, but the underlying brain mechanisms remain underexplored. Especially, the causal contribution of specific patterns of oscillatory activity within the human striatum is unknown. To address this question, we exploited an innovative, non-invasive deep brain stimulation technique called transcranial Temporal Interference Stimulation (tTIS) during reinforcement motor learning with concurrent neuroimaging, in a randomised, sham-controlled, double-blind study. Striatal tTIS applied at 80Hz, but not at 20Hz, abolished the benefits of reinforcement on motor learning. This effect was related to a selective modulation of neural activity within the striatum. Moreover, 80Hz, but not 20Hz tTIS increased the neuromodulatory influence of the striatum on frontal areas involved in reinforcement motor learning. These results show for the first time that tTIS can non-invasively and selectively modulate a striatal mechanism involved in reinforcement learning, opening new horizons for the study of causal relationships between deep brain structures and human behaviour.

1. Introduction

The ability to learn from past outcomes, often referred to as reinforcement learning, is fundamental for complex biological systems[1]. Reinforcement learning has been classically studied in the context of decision making, when agents have to decide between a discrete number of potential options[2]. Importantly, there is an increasing recognition that reinforcement learning processes are also at play in other contexts including during practice of a new motor skill[3–5]. For instance, the addition of reinforcement feedback during motor training can improve motor learning, presumably by boosting the retention of newly acquired motor memories[6,7]. Interestingly, reinforcement feedback also appears to be relevant for the rehabilitation of patients suffering from motor impairments[8–10]. Yet, despite these promising results, there is currently a limited understanding of the brain mechanisms that are critical to implement this behaviour.

A prominent hypothesis in the field is that the striatum, a structure that is particularly active both during reinforcement[11] and motor learning[12], may be causally involved in the beneficial effects of reinforcement on motor learning. As such, the striatum shares dense connexions with dopaminergic structures of the midbrain as well as with pre-frontal and motor cortical regions[13], and is therefore well positioned to mediate reinforcement motor learning[14–16]. This idea is supported by neuroimaging studies showing reward-related activation of the striatum during motor learning[17,18]. More specifically, within the striatum, oscillatory activity in specific frequency bands is suggested to be involved in aspects of reinforcement processing. Previous rodent studies have shown that striatal high gamma oscillations (~ 80 Hz) transiently increase following reward delivery[19–23], but not when reward is withheld[19]. Hence, dynamic changes of high gamma activity in the striatum[19,24,25] and in other parts of the basal ganglia[26,27] may encode the outcome of previous movements (i.e., success or failure) and support learning. Consistent with a role of such oscillatory activity in reinforcement learning, high gamma activity in the striatum shows coherence with frontal cortex oscillations and is up-regulated by dopaminergic agonists[19]. Hence, this body

4

74   of work suggests that reinforcement-related modulation of striatal oscillatory activity, especially in

75   the gamma range, may be crucial for reinforcement learning of motor skills. Conversely, striatal

76   beta oscillations (~20 Hz) have been largely associated with sensorimotor functions[28]. For

77   instance, beta oscillations in the striatum are exacerbated in Parkinson's disease and associated

78   to the severity of motor symptoms[29–31]. Consistently, excessive beta connectivity is reduced by

79   anti-parkinsonian treatment in proportion to the related motor improvement[32]. Taken together,

80   these elements suggest that striatal high gamma and beta activity may have different functional

81   roles preferentially associated to reinforcement and sensorimotor functions, respectively.

82   The studies mentioned above provide associative evidence linking the presence of

83   reinforcement with changes of neural activity within the striatum determined through

84   neuroimaging[17,18], but do not allow to draw conclusions regarding its causal role in reinforcement

85   motor learning in humans. The only causal evidence available to date comes from animal work

86   showing modulation of reinforcement-based decision-making with striatal stimulation[33,34]. A

87   reason for the current absence of investigations of the causal role of the striatum in human

88   behaviour is related to its deep localization in the brain. As such, current non-invasive brain

89   stimulation techniques, such as transcranial magnetic stimulation (TMS) or classical transcranial

90   electric stimulation (tES), do not allow to selectively target deep brain regions, because these

91   techniques exhibit a steep depth-focality trade-off[35,36]. Studies of patients with striatal lesions[37,38]

92   or invasive deep brain stimulation of connected nuclei[39,40] have provided insights into the role of

93   the basal ganglia in reinforcement learning. However, their conclusions are partially limited by the

94   fact that the studied patients also exhibit altered network properties resulting from the underlying

95   pathology (e.g., neurodegeneration, lesions) or from the respective compensatory mechanisms.

96   Here, we address these challenges by exploiting transcranial electric Temporal Interference

97   Stimulation (tTIS), a new non-invasive brain stimulation approach allowing to target deep brain

98   regions in a frequency-specific and focal manner in the physiological state[41,42].

99   The concept of tTIS was initially proposed and validated on the hippocampus of rodents[41]

100   and was then further tested through computational modelling[43–47] and in first applications on

101   cortical areas in humans[48,49]. tTIS requires two pairs of electrodes to be placed on the head, each

102   pair delivering a high frequency alternating current. One key element is that this frequency has to

103   be high enough (i.e., in the kHz range) to avoid direct neuronal entrainment, based on the low-

104   pass filtering properties of neuronal membranes[50]. The second key element is the application of a

105   small difference of frequency between the two alternating currents. The superposition of the

106   electric fields creates an envelope oscillating at this low-frequency difference, which can be

107   steered towards individual deep brain structures (e.g., by optimizing electrodes' placement), and

108   is in a range able to influence neuronal activity [41,51–53]. An interesting feature of tTIS is to stimulate

109   at a particular frequency of interest in order to preferentially interact with specific neuronal

110   processes[41,42]. Importantly, despite these exciting opportunities, current evidence for tTIS-related

111   neuromodulation of deep brain structures, such as the striatum, is lacking in humans.

112   Here, we combine tTIS with electric field modelling for target localisation, behavioural data

113   and functional magnetic resonance imaging (fMRI) to evaluate the causal role of specific patterns

114   of striatal activity in reinforcement learning of motor skills. Based on the studies mentioned above,

115   we hypothesised that striatal tTIS at high gamma frequency ($tTIS_{80Hz}$) would disturb the fine-tuning

116   of high gamma oscillatory activity in the striatum and thereby would perturb reinforcement motor

117   learning in contrast to beta ($tTIS_{20Hz}$) or sham ($tTIS_{Sham}$) stimulation. More specifically, we

118   reasoned that applying a constant high gamma rhythm in the striatum would disturb the temporally

119   precise and reinforcement-specific modulation of high gamma activity. Moreover, given that the

120   stimulation protocol was not individualised to endogenous high gamma activity and not

121   synchronised to ongoing activity in other hubs of the reinforcement learning network (e.g., the

122   frontal cortex), we anticipated disruptive rather than beneficial effects of $tTIS_{80Hz}$.

123   In line with our prediction, we report that $tTIS_{80Hz}$ disrupted motor learning compared to the

124   controls, but only in the presence of reinforcement. To evaluate the potential neural correlates of

125   these behavioral effects, we measured BOLD activity in the striatum and effective connectivity

126   between the striatum and frontal cortical areas involved in reinforcement motor learning. We found

127   that the disruptive effect of $tTIS_{80Hz}$ on reinforcement learning was associated to a specific

128   modulation of BOLD activity in the putamen and caudate, but not in the cortex, supporting the

129   ability of tTIS to selectively modulate striatal activity without affecting overlying cortical areas.

130   Moreover, $tTIS_{80Hz}$ also increased the neuromodulatory influence of the striatum on frontal cortical

131   areas involved in reinforcement motor learning. Overall, the present study shows for the first time

132   that tTIS can non-invasively and selectively modulate a striatal mechanism involved in

133   reinforcement learning opening new horizons for the study of causal relationships between deep

134   brain structures and human behaviour.

7

2. Results

24 healthy participants (15 women, 25.3 ± 0.1 years old; mean ± SE) performed a force tracking task in the MRI with concurrent tTIS of the striatum. The task required participants to modulate the force applied on a hand-grip force sensor in order to track a moving target with a cursor with the right, dominant hand[54,55] (**Figure 1A**). At each block, participants had to learn a new pattern of motion of the target (**Figure S1**; see Methods). In Reinf$_{ON}$ blocks, participants were provided with online reinforcement feedback during training, giving them real-time information about success or failure throughout the trial, indicated as a green or red target, respectively (please see **Video S1** for the task). The reinforcement feedback was delivered according to a closed-loop schedule[8], in which the success criterion to consider a force sample as successful was updated based on the median performance over the 4 previous trials (see Methods for more details). In Reinf$_{OFF}$ blocks, participants practiced with a visually matched random feedback (cyan/magenta). Importantly, in both types of blocks, training was performed with partial visual feedback of the cursor, a condition that has been shown to maximise reinforcement effects in various motor learning paradigms[4,56–58] and which yielded significant effects of reinforcement on motor learning as also demonstrated in an additional behavioural study testing another group of healthy participants on the same task (n = 24, Figure S2). Before and after training, participants performed Pre- and Post-training assessments with full visual feedback, no reinforcement and no tTIS, allowing us to evaluate motor learning. To assess the effect of tTIS on reinforcement-related benefits in motor learning and the associated neural changes, participants performed 6 blocks of 36 trials in the MRI, with concurrent tTIS during training, delivered with a Δf of 20 Hz (tTIS$_{20Hz}$), 80 Hz (tTIS$_{80Hz}$) or as a sham (tTIS$_{Sham}$; 3 tTIS$_{TYPE}$ x 2 Reinf$_{TYPE}$ conditions; **Figure 1B, 1C**). Notably, the order of the conditions was balanced among the 24 participants, ensuring that any potential carry-over effect would have the same impact on each experimental condition. To determine the best electrode montage to stimulate the human striatum (putamen, caudate and nucleus

8

161   accumbens [NAc] bilaterally), computational modelling with a realistic head model was conducted

162   with Sim4Life[59] (see Methods). The selected montage (F3-F4; TP7-TP8) generated a theoretical

163   temporal interference electric field that was ~30-40% stronger in the striatum than in the overlying

164   cortex, reaching magnitudes of 0.5 to 0.6 V/m (**Figure 1D, 1E**).

165
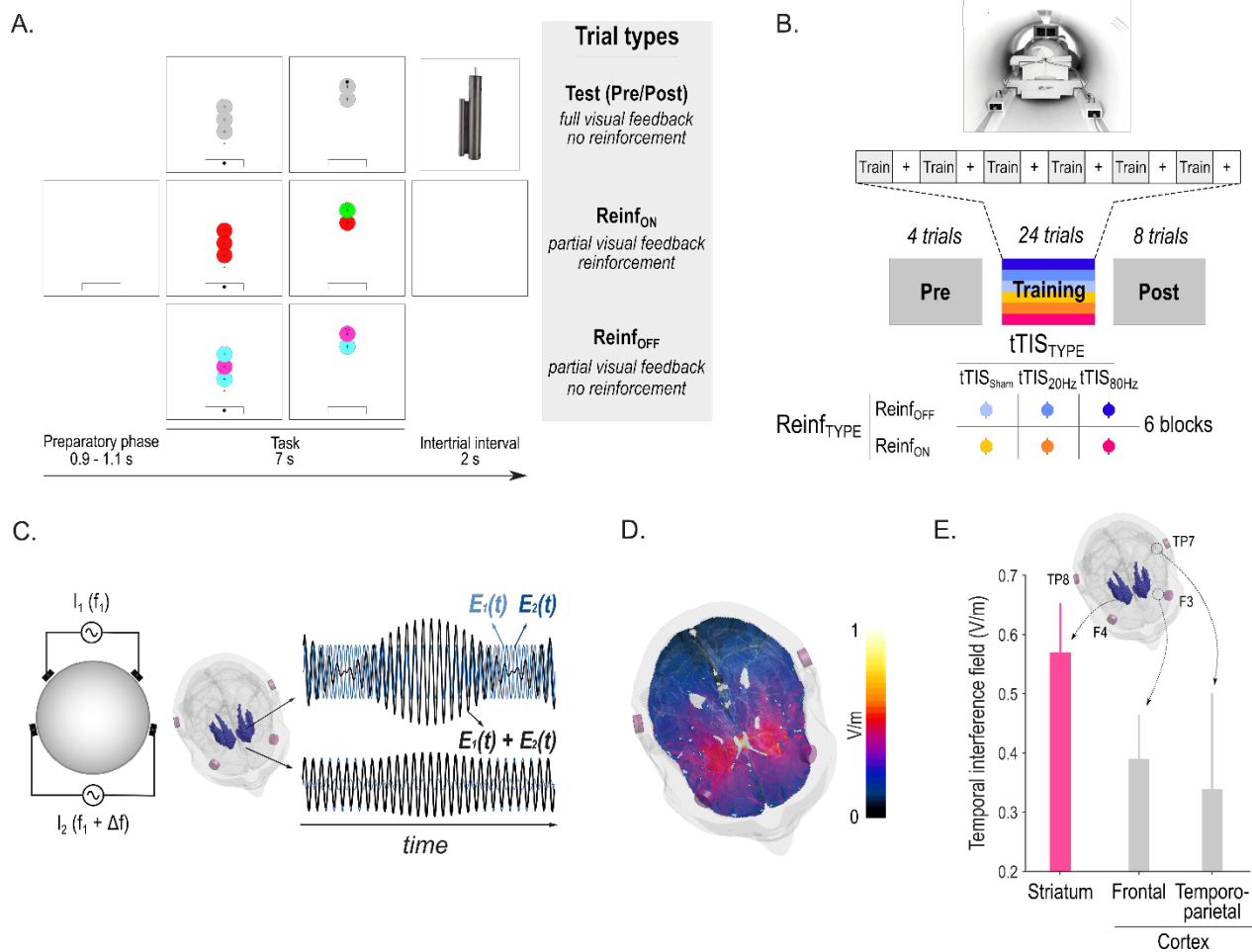
Figure 1. Striatal tTIS during reinforcement learning of motor skills in the MRI. A) Motor learning task. Participants were required to squeeze a hand grip force sensor (depicted in the upper right corner of the figure) in order to track a moving target (larger circle with a cross in the center) with a cursor (black smaller circle)[54,55]. Pre- and Post-training assessments were performed with full visual feedback of the cursor and no reinforcement. In $Reinf_{ON}$ and $Reinf_{OFF}$ trials, participants practiced the task with or without reinforcement feedback, respectively. As such, in $Reinf_{ON}$ trials, the color of the target varied in real-time as a function of the subjects' tracking performance. **B) Experimental procedure.** Participants performed the task in the MRI with concomitant TI stimulation. Blocks of training were composed of 36 trials (4 Pre-, 24 Training and 8 Post-training trials) interspersed with short resting periods (represented as + on the figure). The 6 training types resulted from the combination of 3 $tTIS_{TYPES}$ and 2 $Reinf_{TYPES}$. **C) Concept of tTIS.** On the left, two pairs of electrodes are shown on a head model and currents are applied with a

178 frequency f1 and f1+Δf. On the right, the interference of the two electric fields within the brain is
179 represented for two different locations with respectively high and low envelope modulation. $E_1(t)$
180 and $E_2(t)$ represent the modulation of the fields' magnitude over time. tTIS was delivered either
181 with a Δf of 20 or 80 Hz or as a sham (ramp-up and immediate ramp-down of high frequency
182 currents with flat envelope). **D) Electric field modelling with the striatal montage.** Temporal
183 interference exposure (electric field modulation magnitude). **E) Temporal interference exposure**
184 **averaged in the striatum and in the overlying cortex.** Magnitude of the field in the cortex was
185 extracted from the Brainnetome atlas (BNA[60]) regions underneath the stimulation electrodes (F3-
186 F4 and TP7-TP8). Error bars represent the standard deviation over the voxels in the considered
187 region.

188

189 **tTIS$_{80Hz}$ disrupts reinforcement learning of motor skills**

190 　　　　Task performance was evaluated by means of the Error, which was defined as the absolute

191 difference between the applied and target force averaged across samples for each trial, as done

192 previously[4,54,56] (**Figure 2A**). Across conditions, the Post-training Error was reduced compared to

193 the Pre-training Error (single sample t-test on the normalised Post-training data: $t_{(24)}$=-2.69;

194 p=0.013; Cohen's d=-0.55), indicating significant motor learning during the task (**Figure 2B**). Such

195 improvement was greater when participants had trained with reinforcement (Reinf$_{TYPE}$ effect in the

196 Linear Mixed Model (LMM): $F_{(1, 1062.2)}$=5.17; p=0.023; d=-0.14 for the post-hoc contrast Reinf$_{ON}$ –

197 Reinf$_{OFF}$), confirming the beneficial effect of reinforcement on motor learning[7,58]. Crucially though,

198 this effect depended on the type of stimulation applied during training (Reinf$_{TYPE}$ x tTIS$_{TYPE}$

199 interaction: $F_{(2, 1063.5)}$=2.11; p=0.034; **Figure 2C**). While reinforcement significantly improved

200 learning when training was performed with tTIS$_{Sham}$ (p=0.036; d=-0.22) and tTIS$_{20Hz}$ (p=0.0089;

201 d=-0.27), this was not the case with tTIS$_{80Hz}$ (p=0.43; d=0.083). Consistently, direct between-

202 condition comparisons showed that in the Reinf$_{ON}$ condition, learning was reduced with tTIS$_{80Hz}$

203 compared to tTIS$_{20Hz}$ (p=0.039; d=0.26) and tTIS$_{Sham}$ (p<0.001; d=0.45) but was not different

204 between tTIS$_{20Hz}$ and tTIS$_{Sham}$ (p=0.15; d=0.20). This disruption of motor learning with tTIS$_{80Hz}$ was

205 not observed in the absence of reinforcement (tTIS$_{80Hz}$ vs. tTIS$_{20Hz}$: p=0.59; d=-0.10, tTIS$_{80Hz}$ vs.

206 tTIS$_{Sham}$: p=0.34; d=0.15). These results strongly point to the fact that high gamma striatal tTIS

207   specifically disrupts the benefits of reinforcement on motor learning and not motor learning in

208   general.

209   Although training with $tTIS_{20Hz}$ did not alter the benefits of reinforcement on motor learning,

210   we found that learning without reinforcement was significantly impaired in this condition ($tTIS_{20Hz}$

211   vs. $tTIS_{Sham}$: p=0.046; d=0.25, **Figure 2C**). This suggests that $tTIS_{20Hz}$ may disrupt a qualitatively

212   different mechanism involved in motor learning from sensory feedback[61], in line with the role of

213   striatal beta oscillations in sensorimotor function[28].

214   Next, we evaluated the effect of tTIS on motor performance during training itself. As shown

215   in Figure 2A, the Error was generally higher during Training than in Test trials due to the presence

216   of visual uncertainty during this phase. The extent of this disruption was reduced in the presence

217   of reinforcement ($Reinf_{TYPE}$: $F_{(1,\ 3262.4)}$=339.89; p<0.001; d=-0.64 for the contrast $Reinf_{ON}$ –

218    $Reinf_{OFF}$), demonstrating the ability of subjects to exploit real-time reinforcement information to

219   improve tracking (**Figure 2D**). Notably, this effect was not modulated by $tTIS_{TYPE}$ ($Reinf_{TYPE}$ x

220    $tTIS_{TYPE}$: $F_{(2,\ 3265.8)}$=0.91; p=0.40), indicating that tTIS did not directly influence reinforcement gains

221   during tracking. Interestingly though, striatal stimulation did impact on general tracking

222   performance independently of reinforcement as indicated by a significant $tTIS_{TYPE}$ effect ($tTIS_{TYPE}$:

223    $F_{(2,\ 3262.4)}$=42.85; p<0.001). This effect was due to an increase in the Error when $tTIS_{20Hz}$ was

224   applied (p<0.001; d=0.28 when compared to $tTIS_{Sham}$), which was even stronger during $tTIS_{80Hz}$

225   (p<0.001; d=0.38 and p=0.031; d=0.11 when compared to $tTIS_{Sham}$ and $tTIS_{20Hz}$, respectively). An

226   additional analysis showed that the detrimental effect of tTIS on motor performance was actually

227   due to an impaired ability to improve performance during Training (LMM with continuous fixed

228   effect Trial: $tTIS_{TYPE}$ x Trial interaction: $F_{(2,\ 3399)}$=4.46; p=0.012, post-hoc tests: $tTIS_{Sham}$ vs. $tTIS_{20Hz}$:

229   p=0.013; $tTIS_{Sham}$ vs. $tTIS_{80Hz}$: p=0.068; $tTIS_{20Hz}$ vs. $tTIS_{80Hz}$: p=0.81; **Figure S3**). However, again,

230   this effect did not depend on the presence of reinforcement ($Reinf_{TYPE}$ x $tTIS_{TYPE}$ x Trial: $F_{(2,}$

231    $_{3399)}$=0.51; p=0.60). Notably, we also found that the detrimental effect of striatal tTIS did not depend

232 on the availability of visual information on the cursor, but rather that tTIS had a general effect on

233 motor performance irrespective of visual and reinforcement feedback (see Supplementary

234 materials). This analysis also confirmed that reinforcement gains in motor performance were

235 stronger when visual information was not available (**Figure S4**), in line with the behavioural data

236 mentioned above (Figure S2) and previous studies[57,62]. Overall, these results suggest that striatal

237 tTIS altered motor performance in a frequency-dependent manner but did not influence the ability

238 to rapidly adjust motor commands based on reinforcement feedback during training. Hence,

239 $tTIS_{80Hz}$ may not disrupt real-time processing of reinforcement feedback, but may rather impair the

240 beneficial effect of reinforcements on the retention of motor memories[6,7].

241   Notably, these effects could not be explained by potential differences in initial performance

242 between conditions ($Reinf_{TYPE}$ x $tTIS_{TYPE}$: $F_{(2, 519.99)}$=1.08; p=0.34), nor by changes in the flashing

243 properties of the reinforcement feedback (i.e., the frequency of color change during tracking;

244 $Reinf_{TYPE}$ x $tTIS_{TYPE}$: $F_{(2, 3283)}$=0.19; p=0.82), or by differences in success rate in the $Reinf_{ON}$ blocks

245 (i.e., the proportion of success feedback during tracking; $tTIS_{TYPE}$: $F_{(2, 1702)}$=0.17; p=0.84). The

246 $Reinf_{TYPE}$ x $tTIS_{TYPE}$ effect on learning was also not influenced by the order of the reinforcement

247 conditions (analysis on sub-groups based on whether participants experienced $Reinf_{ON}$ or $Reinf_{OFF}$

248 first; no $Reinf_{TYPE}$ x $tTIS_{TYPE}$ x $Group_{TYPE}$ interaction: $F_{(2,1105.06)}$=1.75; p=0.17; see Supplementary

249 materials for more details on these analyses).

250   Finally, we confirmed that these results were not a consequence of an inefficient blinding.

251 As such, when debriefing after the experiment, only 6/24 participants were able to successfully

252 identify the order of the stimulation applied (e.g., real – real – placebo; chance level: 4/24; Fisher

253 exact test on proportions: p=0.74). Consistently, the magnitude (**Figure S5A**) and type (**Figure**

254 **S5B**) of tTIS-evoked sensations evaluated before the experiment were qualitatively similar across

255 conditions and tTIS was generally well tolerated in all participants (no adverse events reported).

256 This suggests that blinding was successful and is unlikely to explain our findings. More generally,

257   this is a first indication that tTIS evokes very limited sensations (e.g., only 2/24 and 1/24 subjects

258   rated sensations evoked at 2 mA as "strong" for tTIS$_{20Hz}$ and tTIS$_{80Hz}$, respectively; **Figure S5A**)

259   that are compatible with efficient blinding.

260
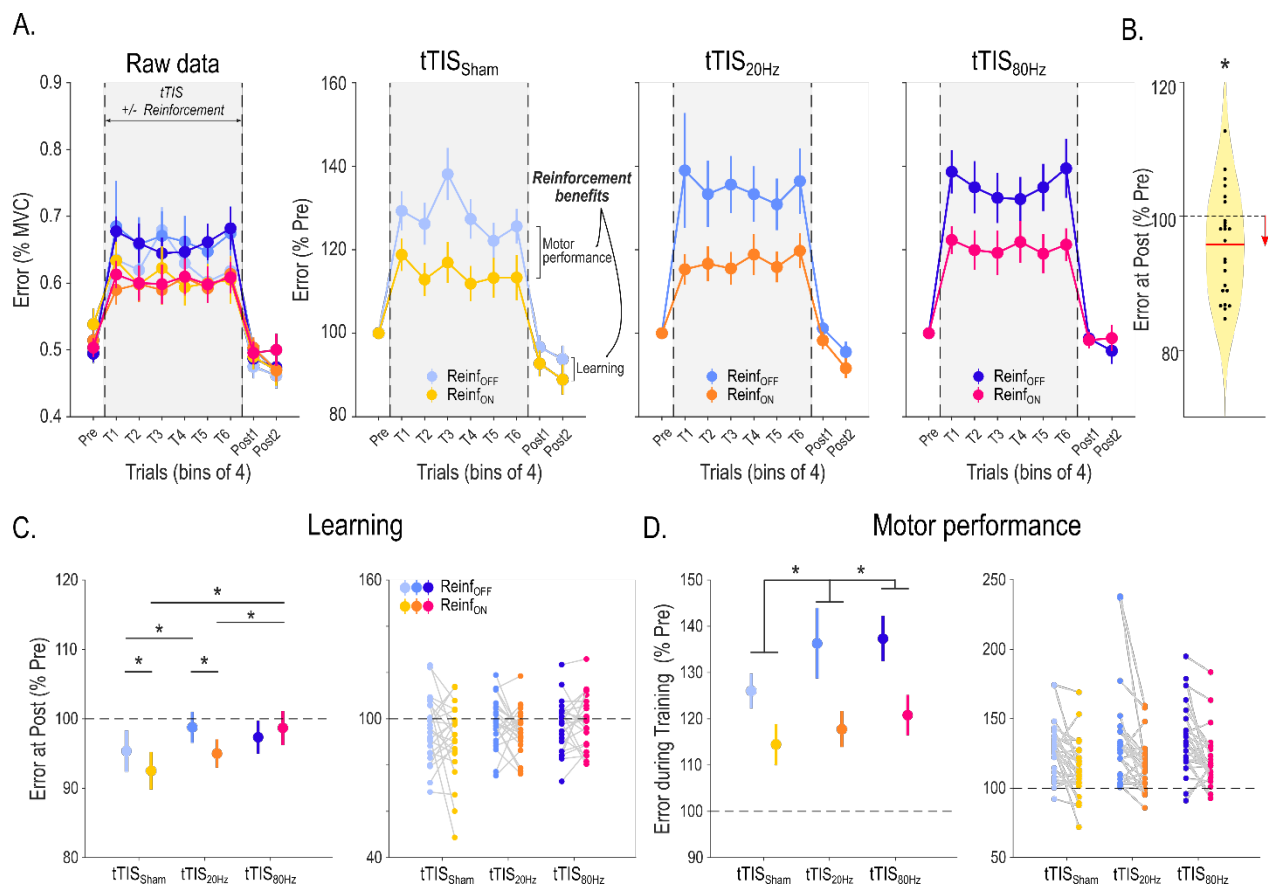
Figure 2. Behavioural results. A) Motor performance across training. Raw Error data
(expressed in % of Maximum Voluntary Contraction [MVC]) are presented on the left panel for the
different experimental conditions in bins of 4 trials. The increase in Error during Training is related
to the visual uncertainty (i.e., intermittent disappearance of the cursor) that was applied to enhance
reinforcement effects. On the right, the three plots represent the Pre-training normalised Error in
the tTIS$_{Sham}$, tTIS$_{20Hz}$ and tTIS$_{80Hz}$ blocks. Reinforcement-related benefits represent the
improvement in the Error measured in the Reinf$_{ON}$ and Reinf$_{OFF}$ blocks, during Training (reflecting
benefits in motor performance) or at Post-training (reflecting benefits in learning). **B) Averaged
learning across conditions.** Violin plot showing the Error distribution at Post-training (expressed
in % of Pre-training) averaged across conditions, as well as individual subject data. A single-
sample t-test showed that the Post-training Error was reduced compared to the Pre-training level,
indicating significant learning in the task. **C) Motor learning.** Averaged Error at Post-training
(normalised to Pre-training) and the corresponding individual data points in the different
experimental conditions are shown on the left and right panels, respectively, for the subjects
included in the analysis (i.e., after outlier detection, remaining n=23). Reduction of Error at Post-
training reflects true improvement at tracking the target in Test conditions (in the absence of
reinforcement, visual uncertainty or tTIS). The LMM ran on these data revealed a specific effect

13

278   of $tTIS_{80Hz}$ on reinforcement-related benefits in learning. **D) Motor performance.** Averaged Error
279   during Training (normalised to Pre-training) and the corresponding individual data points in the
280   different experimental conditions are shown on the left and right panels, respectively, for the
281   subjects included in the analysis (i.e., after outlier detection, n=23). Individual data points are
282   shown on the right panel. Error change during Training reflect the joint contribution of the
283   experimental manipulations (visual uncertainty, potential reinforcement and tTIS) on motor
284   performance. The LMM ran on these data showed a frequency-dependent effect of tTIS on motor
285   performance, irrespective of reinforcement. *: $p<0.05$. Data are represented as mean ± SE.

286

287   The effect of $tTIS_{80Hz}$ on reinforcement motor learning is related to modulation of neural

288   activity in the striatum

289   As mentioned above, task-based fMRI was acquired during Training with concomitant tTIS.

290   This allowed us to evaluate the neural effects of tTIS and their potential relationship to the

291   behavioural effects reported above. As a first qualitative evaluation of the data, we performed a

292   whole-brain analysis in the $tTIS_{Sham}$ condition to assess the network activated during reinforcement

293   motor learning ($Reinf_{ON}$ condition). Consistent with previous neuroimaging studies employing

294   similar tasks[63,64], we found prominent BOLD activations in a motor network including the putamen,

295   thalamus, cerebellum and sensorimotor cortex, particularly on the left hemisphere, contralateral

296   to the trained hand (**Figure S6, Table S2**). Notably though, contrasting $Reinf_{ON}$ and $Reinf_{OFF}$

297   conditions did not reveal any significant cluster at the whole-brain level. Hence, this first analysis

298   did not reveal any region specifically activated in the presence of reinforcement, but rather

299   confirms the involvement of a motor network engaged in this type of task irrespective of the

300   reinforcement feedback.

301   As a second step, we evaluated the effect of tTIS on striatal activity, as a function of the

302   type of reinforcement feedback and focusing on the very same regions of interest (ROI) that were

303   used to optimise tTIS exposure in the modelling. Based on this, we extracted averaged BOLD

304   activity within the bilateral putamen, caudate and NAc based on the Brainnetome atlas (BNA^{60}),

305   in the different experimental conditions and considered these six striatal ROIs (ROI_{STR}) as fixed

306   effects in the LMM. This model revealed a strong enhancement of striatal activity with $Reinf_{ON}$ with

307   respect to $Reinf_{OFF}$ ($F_{(1, 800.01)}$=13.23; p<0.001; d=0.25 for the contrast $Reinf_{ON}$ – $Reinf_{OFF}$)

308   consistent with previous literature[11], but no $tTIS_{TYPE}$ effect ($F_{(2, 800.01)}$=0.46; p=0.63) and no

309   interaction (all p> 0.65; **Figure 3A**). Despite the absence of effects of tTIS on averaged striatal

310   activity, we then asked whether the behavioural effects of $tTIS_{80Hz}$ on reinforcement motor learning

311   (i.e., $tTIS_{80Hz}$ vs. $tTIS_{20Hz}$ and $tTIS_{Sham}$ with $Reinf_{ON}$) could be linked to modulation of activity in core

312   brain regions. To do so, we ran a whole-brain analysis focusing on the main behavioural effects

313   mentioned above. Results revealed that the effect of $tTIS_{80Hz}$ (with respect to $tTIS_{20Hz}$) on motor

314   learning in the $Reinf_{ON}$ condition was specifically related to modulation of activity in two clusters

315   encompassing the left putamen and bilateral caudate (**Figure 3B, Table S3**). Notably, the

316   presence of the high frequency carrier (kHz) in both stimulation conditions rules out the possibility

317   that the correlation was due to putative neuromodulatory effects of high frequency stimulation. No

318   significant clusters were found neither for the $tTIS_{80Hz}$ – $tTIS_{Sham}$ contrast, nor for the control

319    $tTIS_{20Hz}$ - $tTIS_{Sham}$ contrast, indicating that the reported correlation is not due to a general link

320   between striatal activity and reinforcement motor learning. Overall, these results provide evidence

321   that the detrimental effect of $tTIS_{80Hz}$ on reinforcement learning of motor skills is related to

322   modulation of neural activity specifically in the striatum.

15

A.

B.
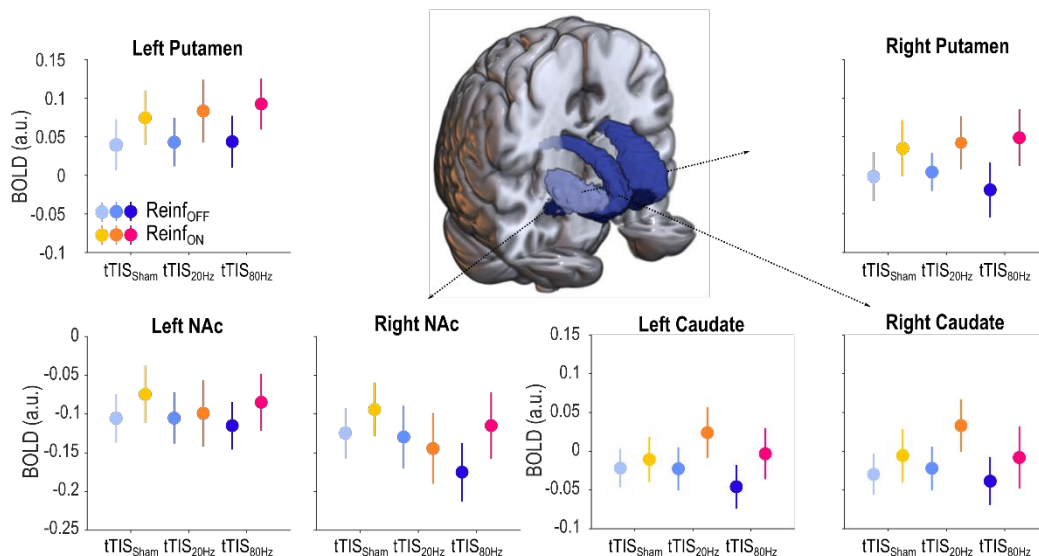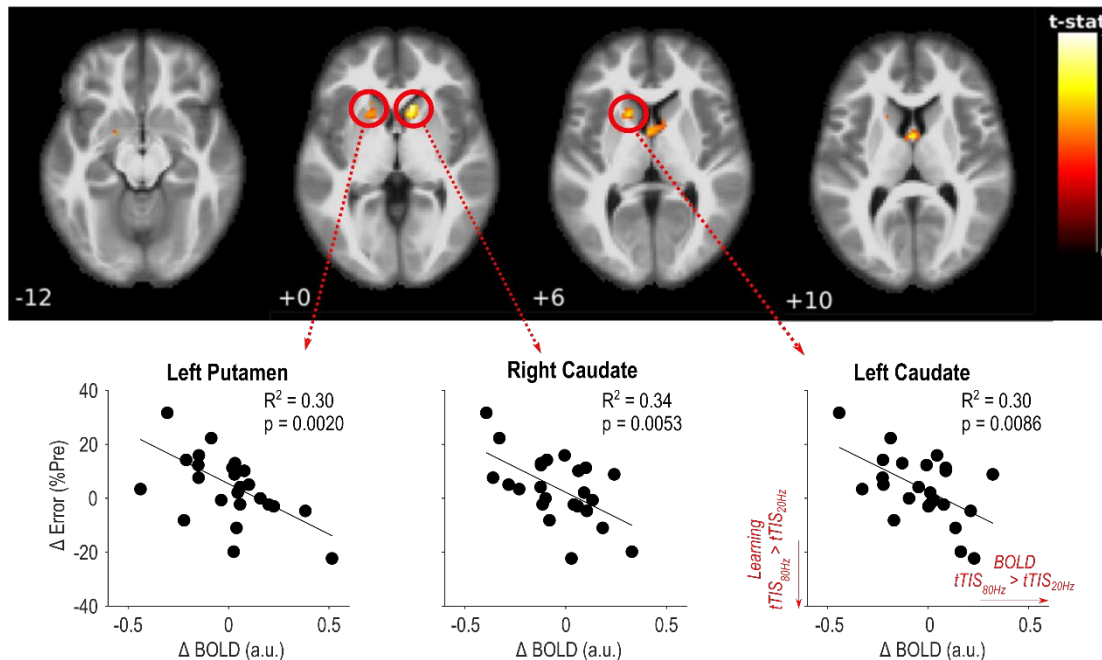
Figure 3. Striatal activity. A) Striatal BOLD responses. A 3D-reconstruction of the striatal masks used in the current experiment is surrounded by plots showing averaged BOLD activity for each mask in the different experimental conditions. A LMM ran on these data showed higher striatal responses in the Reinf$_{ON}$ with respect to the Reinf$_{OFF}$ condition, but no effect of tTIS$_{TYPE}$ and no interaction. **B) Whole-brain activity associated to the behavioural effect of tTIS$_{80Hz}$ on reinforcement motor learning.** Correlation between tTIS-related modulation of striatal activity (tTIS$_{80Hz}$ – tTIS$_{20Hz}$) and learning abilities in the Reinf$_{ON}$ condition. Significant clusters of correlation were found in the left putamen and bilateral caudate (uncorrected voxel-wise FWE: p=0.001, and corrected cluster-based FDR: p=0.05). Lower panel shows individual correlations for the three significant regions highlighted in the whole-brain analysis. *: p<0.05. Data are represented as mean ± SE.

16

tTIS$_{80Hz}$ enhances effective connectivity between the striatum and frontal cortex.

Interactions between the striatum and frontal cortex are crucial for a variety of behaviours including motor and reinforcement learning[13]. In particular, reinforcement motor learning requires to use information about task success to guide future motor commands[4], a process for which the striatum may play an integrative role at the interface between fronto-striatal loops involved in reward processing and motor control[13,65]. In a subsequent analysis, we asked whether striatal tTIS modulates striatum to frontal cortex communication during reinforcement motor learning. More specifically, we computed effective connectivity (using the generalized psychophysiological interactions method[66]) between striatal and frontal regions classically associated with motor and reward-related functions, and thought to be involved in reinforcement motor learning[67,68]. For the motor network, we evaluated effective connectivity between motor parts of the striatum (i.e., dorso-lateral putamen (dlPu) and dorsal caudate (dCa)) and two regions strongly implicated in motor learning: the medial part of the supplementary motor area (SMA) and the part of the primary motor cortex (M1) associated to upper limb functions (**Figure 4A**). For the reward network, we assessed connectivity between parts of the striatum classically associated to limbic functions (i.e., the NAc and the ventro-medial putamen (vmPu) and two frontal areas involved in reward processing: the anterior cingulate cortex (ACC) and the ventro-medial prefrontal cortex (vmPFC; **Figure 4B**; [11]). The LMM ran with the fixed effects Reinf$_{TYPE}$, tTIS$_{TYPE}$ and Network$_{TYPE}$ showed a significant effect of tTIS$_{TYPE}$ ($F_{(2, 2264.0)}$=5.42; p=0.0045), that was due to higher connectivity in the tTIS$_{80Hz}$ condition with respect to tTIS$_{Sham}$ (p=0.0038; d=0.16) and tTIS$_{20Hz}$ (at the trend level, p=0.069; d=0.11). There was no difference in connectivity between tTIS$_{20Hz}$ and tTIS$_{Sham}$ (p=0.58; d=0.051). Hence, tTIS$_{80Hz}$, but not tTIS$_{20Hz}$, enhanced effective connectivity between the striatum and frontal cortex during motor training. This increase in effective connectivity with tTIS$_{80Hz}$ actually led to a connectivity closer to the resting state (values closer to 0, see Methods). Put differently, while the task induced

17

360   a reduction in effective connectivity between striatum and frontal cortex, $tTIS_{80Hz}$ disrupted this

361   modulation by bringing connectivity back to the resting state.

362   The LMM did not reveal any effect of $Reinf_{TYPE}$ ($F_{(1, 2264.0)}$=0.010; p=0.92), $Network_{TYPE}$ ($F_{(1,}$

363    $_{2264.0)}$=3.16; p=0.076) and no double interaction (note the trend for a $Reinf_{TYPE}$ x $Network_{TYPE}$ effect

364   though: $F_{(1, 2264.0)}$=3.52; p=0.061). Yet, we did find a significant $Reinf_{TYPE}$ x $tTIS_{TYPE}$ x $Network_{TYPE}$

365   interaction ($F_{(2, 2264.0)}$=4.87; p=0.0078). Such triple interaction was related to the fact that $tTIS_{80Hz}$

366   increased connectivity in the $Reinf_{ON}$ condition in the motor network ($Reinf_{ON}$ vs. $Reinf_{OFF}$:

367   p=0.0012; d=0.33; Figure 4A), while it tended to have the opposite effect in the reward network

368   (p=0.063; d=-0.19; Figure 4B). This increase was not present in any of the two networks when

369   either $tTIS_{Sham}$ or $tTIS_{20Hz}$ were applied (all p> 0.40). Moreover, in the motor network, connectivity

370   in the $Reinf_{ON}$ condition was higher with $tTIS_{80Hz}$ than with $tTIS_{Sham}$ (p<0.001; d=0.42) and $tTIS_{20Hz}$

371   (at the trend level; p=0.059; d=0.23, Figure 4A). These data suggest that $tTIS_{80Hz}$ enhanced the

372   neuromodulatory influence of the striatum on motor cortex during task performance, but only in

373   the presence of reinforcement. In the reward network, post-hocs revealed that connectivity in the

374    $Reinf_{OFF}$ condition was significantly higher with $tTIS_{80Hz}$ compared to $tTIS_{20Hz}$ (p=0.045; d=0.25;

375   Figure 4B), in line with the general effect of $tTIS_{TYPE}$ on connectivity reported above. This pattern

376   of results suggests that the increase of connectivity from striatum to frontal cortex observed with

377    $tTIS_{80Hz}$ depends on the presence of reinforcement, in particular in the motor network. Such

378   reinforcement-dependent increase of connectivity may reflect the preferential effect of $tTIS_{80Hz}$ on

379   striatal gamma oscillations[69] in a situation where these oscillations are already boosted by the

380   presence of reinforcement[19] (see Discussion).

381   In a subsequent analysis, we verified that these results did not depend on the specific

382   frontal ROIs considered in the analysis (ROI_{TYPE}: M1 and SMA in the motor network and ACC and

383   vmPFC in the reward network). Importantly, we did not find a $tTIS_{TYPE}$ x $Reinf_{TYPE}$ x ROI_{TYPE}

384   interaction neither in the motor ($F_{(2,1112)}$=0.83; p=0.44) nor in the reward network ($F_{(2,1112)}$=0.61;

385   p=0.54), suggesting that the main connectivity results were consistent within a network and were

386   not influenced by the specific frontal ROI included in the analysis (see Supplementary materials

387   for more details on this analysis). As an additional control, we verified that the effects of $tTIS_{TYPE}$

388   on connectivity could not be observed in a control network associated to language (as defined by

389   [70]), which was unlikely to be involved in the present task and did not include the striatum (see

390   Methods). As expected, effective connectivity within the language network was not modulated by

391    $Reinf_{TYPE}$ ($F_{(1, 547)}$=0.81; p=0.37), nor by $tTIS_{TYPE}$ ($F_{(2, 547)}$=0.58; p=0.56), or by $Reinf_{TYPE}$ x $tTIS_{TYPE}$

392   ($F_{(2, 547)}$=0.45; p=0.64). Hence, tTIS and reinforcement-related changes in connectivity were

393   consistent within the considered fronto-striatal networks and not observed in a control network

394   unrelated to the task.

395   Notably, contrary to the BOLD results presented above, we did not find any correlations

396   between the effects of $tTIS_{80Hz}$ on connectivity and motor learning, neither in the motor (robust

397   linear regression: $tTIS_{80Hz}$ – $tTIS_{Sham}$: R^2=0.019; p=0.48; $tTIS_{80Hz}$ – $tTIS_{20Hz}$: R^2=0.034; p=0.54) nor

398   in the reward ($tTIS_{80Hz}$ – $tTIS_{Sham}$: R^2=0.037; p=0.46; $tTIS_{80Hz}$ – $tTIS_{20Hz}$: R^2<0.001; p=0.75)

399   network, suggesting some degree of independence between the effect of $tTIS_{80Hz}$ on

400   reinforcement motor learning and on effective connectivity.

401   Overall, these results highlight the ability of $tTIS_{80Hz}$, but not $tTIS_{20Hz}$, to modulate striatum

402   to frontal cortex connectivity, depending on the presence of reinforcement. However, the absence

403   of correlation with the behaviour suggests that this effect may not be directly associated to the

404   detrimental effect of $tTIS_{80Hz}$ on reinforcement motor learning or that $tTIS_{80Hz}$-related changes in

405   striato-frontal communication were linked to other aspects of reinforcement learning not captured

406   by our task.
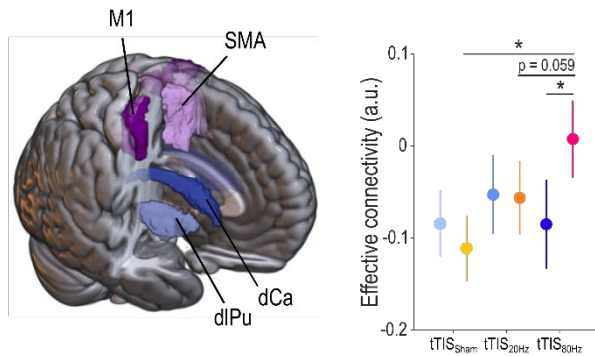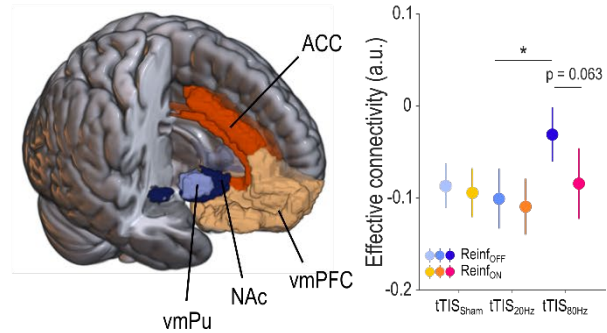
Figure 4. Striatum to frontal cortex effective connectivity. A) Motor network. On the left, 3D reconstruction of the masks used for the motor network (i.e., dorso-lateral putamen, dorsal caudate, M1, SMA). On the right, plot showing effective connectivity from motor striatum to motor cortex in the different experimental conditions. Note the increase of connectivity with $tTIS_{80Hz}$ in the presence of reinforcement. **B) Reward network.** On the left, 3D reconstruction of the masks used for the reward network (i.e., ventro-medial putamen, NAc, vmPFC, ACC). On the right, plot showing effective connectivity from motor striatum to motor cortex in the different experimental conditions. ROIs were defined based on the BNA atlas[12] *: $p < 0.05$. Data are represented as mean ± SE.

20

Neural effects of tTIS$_{80Hz}$ depend on impulsivity

Determining individual factors that shape responsiveness to non-invasive brain stimulation approaches is a crucial step to better understand the mechanisms of action but also to envision stratification of patients in future clinical interventions[71]. A potential factor that could explain inter-individual differences in responsiveness to tTIS$_{80Hz}$ is the level of impulsivity. As such, impulsivity has been associated to changes of gamma oscillatory activity in the striatum of rats[72] and to the activity of fast-spiking interneurons in the striatum[73,74], a neuronal population that is strongly entrained to gamma rythms[19,21] and may therefore be particularly sensitive to tTIS$_{80Hz}$. In a subsequent exploratory analysis, we asked if the neural effects of tTIS$_{80Hz}$ were associated to impulsivity levels, as evaluated by a well-established independent delay-discounting questionnaire performed at the beginning of the experiment[75,76]. Strikingly, a whole-brain analysis revealed that impulsivity was associated to the effect of tTIS$_{80Hz}$ on BOLD activity (with respect to tTIS$_{20Hz}$) specifically in the left caudate nucleus (**Figure S7A, S7B, Table S4**). Moreover, the effect of tTIS$_{80Hz}$ on striatum to motor cortex connectivity reported above was negatively correlated to impulsivity both when contrasting tTIS$_{80Hz}$ with tTIS$_{Sham}$ (**Figure S7C, left**) and with tTIS$_{20Hz}$ (**Figure S7C, middle**). Such correlations were absent when contrasting tTIS$_{20Hz}$ with tTIS$_{Sham}$ (**Figure S7C, right**), as well as when considering the same contrasts in the reward instead of the motor network (see Supplementary materials for more details). Taken together, these results suggest that inter-individual variability in impulsivity might influence the neural responses to striatal tTIS$_{80Hz}$.

3. Discussion

In this study, we combined striatal tTIS with electric field modelling, behavioural and fMRI analyses to evaluate the causal role of the striatum in reinforcement learning of motor skills in healthy humans. $tTIS_{80Hz}$, but not $tTIS_{20Hz}$, disrupted the ability to learn from reinforcement feedback. This behavioural effect was associated to modulation of neural activity specifically in the striatum. As a second step, we show that $tTIS_{80Hz}$, but not $tTIS_{20Hz}$, increased the neuromodulatory influence of the striatum on connected frontal cortical areas involved in reinforcement motor learning. Finally, inter-individual variability in the neural effects of $tTIS_{80Hz}$ could be partially explained by impulsivity, suggesting that this trait may constitute a determinant of responsiveness to high gamma striatal tTIS. Overall, the present study shows for the first time that striatal tTIS can non-invasively modulate a striatal mechanism involved in reinforcement learning, opening new horizons for the study of causal relationships between deep brain structures and human behaviour.

We investigated the causal role of the human striatum in reinforcement learning of motor skills in healthy humans; a question that cannot be addressed with conventional non-invasive brain stimulation techniques. In particular, by stimulating at different frequencies, we aimed at dissociating striatal mechanisms involved in reinforcement and sensorimotor learning. In line with our main hypothesis, we found that striatal $tTIS_{80Hz}$ altered reinforcement learning of a motor skill. Such disruption was frequency- and reinforcement-specific: learning was not altered with striatal $tTIS_{20Hz}$ in the presence of reinforcement, or when striatal $tTIS_{80Hz}$ was delivered in the absence of reinforcement. The rationale to stimulate at high gamma frequency was based on previous work showing reinforcement-related modulation of gamma oscillations in the striatum[19–21,24,26,72,77] and in the frontal cortex[77–80]. Several neuronal mechanisms may contribute to the detrimental effect of $tTIS_{80Hz}$ on reinforcement motor learning. First, as $tTIS_{80Hz}$ consisted in a constant high gamma

462   oscillating field applied on the striatum, it may have perturbed the encoding of reinforcement

463   information into high gamma oscillations[19–21,25–27], preventing participants to learn the motor skill

464   based on different outcomes. Put differently, $tTIS_{80Hz}$ may specifically saturate high gamma activity

465   in the striatum preventing reinforcement-related modulations[81]. Moreover, because reinforcement

466   motor learning likely engages synchronised activity in a network of regions including fronto-striatal

467   loops, neuromodulation of a single node of the circuit may alter synchronisation of activity in the

468   network[81] and the temporal coordination with interacting rhythms[25]. Finally, because we did not

469   have access to electrophysiological recordings of oscillatory activity in the striatum, the applied

470   stimulation was not personalised as it did not take into account the individual high gamma

471   frequency peak associated to reward processing and the potential heterogeneity of gamma activity

472   within the striatum[24]. Hence, $tTIS_{80Hz}$ may have resulted in a frequency mismatch between the

473   endogenous high gamma activity and the externally imposed rhythm, that could paradoxically

474   result in a reduction of neuronal entrainment, in particular when the frequency mismatch is

475   relatively low[82]. Importantly, in contrast to striatal $tTIS_{80Hz}$, we found that $tTIS_{20Hz}$ reduced learning,

476   but only in the absence of reinforcement. This result fits well with the literature linking striatal beta

477   oscillations to sensorimotor functions[28,29,31,83–85]. Taken together, an interpretation of these results

478   is that different oscillations within the striatum support qualitatively distinct motor learning

479   mechanisms with beta activity contributing mostly to sensory-based learning and high gamma

480   activity being particularly important for reinforcement learning. This being said, it is important to

481   note that because we do not have concurrent electrophysiological recordings within the striatum,

482   we cannot be sure that the effects of $tTIS_{20Hz}$ and $tTIS_{80Hz}$ were related to frequency-specific

483   interactions with beta or high gamma rhythms respectively, or rather resulted from different

484   broadband responses when stimulating at these frequencies. Yet, these results still suggest that

485   sensory- and reinforcement-based motor learning rely on partially different neural mechanisms, in

486   line with previous literature[8,9,61,68,86,87].

23

487   Interestingly, striatal tTIS also impaired tracking performance during training, irrespective

488   of the presence of reinforcement. This frequency-dependent reduction of motor performance may

489   be due to altered neuronal processing in the sensorimotor striatum that may lead to less fine-tuned

490   motor control abilities[88]. Importantly though, tTIS did not modulate the ability of participants to

491   benefit from real-time reinforcement feedback during motor performance. This suggests that

492   striatal $tTIS_{80Hz}$ altered the beneficial effects of reinforcement on learning (as evaluated in Test

493   conditions at Post-training), but not on motor performance (as evaluated during Training). Such

494   dissociation between the effects of striatal $tTIS_{80Hz}$ on reinforcement-related gains in motor

495   performance and learning may be explained by the fact that these two phases of the protocol

496   probe different processes[7,54,56,89–91]. While improvement of motor performance with reinforcement

497   relies on rapid feedback corrections based on expected outcomes[67,92–95], reinforcement gains in

498   learning (i.e., probed in Test conditions without reinforcement) may rather reflect the beneficial

499   effect of reinforcement on the retention of motor memories[5,7,54,90]. This idea that mechanisms

500   underlying performance changes in training and retention phases are partially different is well

501   supported by previous motor learning literature[6,8,96]. For instance, in sensorimotor adaptation

502   paradigms, the presence of reward boosts motor memory retention but not the adaptation process

503   itself[7,97], and M1 transcranial direct current stimulation modulates the effect of reward on retention

504   but has no effect on the training phase[90]. Hence, a potential explanation for the present results is

505   that striatal $tTIS_{80Hz}$ did not disrupt rapid motor corrections based on recent outcomes during

506   training, but may rather alter the strengthening of the memory trace based on reinforcements[6,7].

507   Overall, these results are compatible with the view that specific patterns of oscillatory activity in

508   the striatum are involved in motor control and learning processes[31], and can be modulated with

509   electrical stimulation[69,98,99].

510   To better understand the neural effects and frequency-specificity of tTIS, we coupled

511   striatal tTIS and task performance with simultaneous fMRI acquisition. The imaging results support

512   the view that the effect of $tTIS_{80Hz}$ on reinforcement learning of motor skills was indeed related to

513   neuromodulation of the striatum. As such, when considering averaged BOLD activity, we found a

514   general increase of striatal activity when reinforcement was provided[11], but no effect of tTIS.

515   Crucially though, the detrimental effect of $tTIS_{80Hz}$ on reinforcement learning was related to a

516   specific modulation of activity in the caudate and putamen, providing evidence that the present

517   behavioural effects were indeed driven by focal neuromodulation of the striatum (Figure 3).

518   Interestingly, participants with stronger disruption of reinforcement learning at the behavioural

519   level were also the ones exhibiting stronger suppression of striatal activity with $tTIS_{80Hz}$ (compared

520   to $tTIS_{20Hz}$), suggesting that tTIS-induced reduction of striatal activity is detrimental for

521   reinforcement motor learning. Further analyses showed that $tTIS_{80Hz}$, but not $tTIS_{20Hz}$, increased

522   the neuromodulatory influence of the striatum on frontal areas known to be important for motor

523   learning and reinforcement processing[96,100]. More specifically, $tTIS_{80Hz}$ disrupted the task-related

524   decrease in connectivity observed with $tTIS_{Sham}$ and $tTIS_{20Hz}$, bringing connectivity closer to

525   resting-state values. Interestingly, this effect depended on the type of network considered (reward

526   vs. motor) and on the presence of reinforcement. Striatal $tTIS_{80Hz}$ coupled with reinforcement

527   increased connectivity between the motor striatum and the motor cortex while it tended to have

528   the opposite effect when considering the connectivity between limbic parts of the striatum and pre-

529   frontal areas involved in reward processing (Figure 4). This result may reflect the differential

530   influence of striatal tTIS on distinct subparts of the striatum, depending on their pattern of activity

531   during the task[52]. As such, a recent study in non-human primates showed that tACS can have

532   opposite effects on neuronal activity based on the initial entrainment of neurons to the target

533   frequency[82]. Hence, the present differential effects of $tTIS_{80Hz}$ on motor and reward striato-frontal

534   pathways may be due to different initial patterns of activity in these networks in the presence of

535   reinforcement. Electrophysiological recordings with higher temporal resolution than fMRI are

536   required to confirm or infirm this hypothesis. Overall, the present neuroimaging results support the

25

idea that the behavioural effects of striatal $tTIS_{80Hz}$ on reinforcement learning are associated to a selective modulation of striatal activity that influences striato-frontal communication.

The fact that we observed increased connectivity with $tTIS_{80Hz}$ and at the same time a disruption of behaviour may appear contradictory at first glance. Yet, multiple lines of evidence indicate that increases in connectivity are not necessarily beneficial for behaviour. For instance, the severity of motor symptoms in Parkinson's disease is associated with excessive connectivity in the beta band and reduction of such connectivity with treatment is associated to clinical improvement[29,32]. Moreover, there is evidence that excessive functional[101,102] as well as structural[103,104] connectivity in fronto-striatal circuits is associated to impulsivity. Hence, the increase in connectivity observed with $tTIS_{80Hz}$ appears to be compatible with the behavioural findings. This being said, contrary to the BOLD results, we did not find any correlation between the effects of $tTIS_{80Hz}$ on connectivity and on reinforcement motor learning, suggesting some degree of independence between these two effects. Future studies could aim at determining if $tTIS_{80Hz}$-related changes in striato-frontal communication are linked to other aspects of reward processing, not captured by our reinforcement motor learning task.

From a methodological point of view, the present results provide new experimental support to the idea that the effects of tTIS are related to amplitude modulation of electric fields deep in the brain and not to the high frequency fields themselves, in line with recent work[41,42,52]. As such, the different behavioural and neural effects of striatal $tTIS_{80Hz}$ and $tTIS_{20Hz}$ despite comparable carrier frequencies (centered on 2kHz) indicate that temporal interference was indeed the driving force of the present effects. Moreover, disruption of reinforcement motor learning with $tTIS_{80Hz}$ (relative to $tTIS_{20Hz}$) was specifically related to neuromodulation of the striatum, where the amplitude of the tTIS field was highest according to our simulations (see [51,53] for recent validations of comparable simulations in cadavers experiments). Hence, we believe that the frequency- and reinforcement-dependent tTIS effects reported here cannot be explained by direct modulation of neural activity

26

562   by the high frequency fields. Yet, disentangling the neural effects of the low-frequency envelope

563   and the high frequency carrier appears as an important next step to better characterise the

564   mechanisms underlying tTIS[47]. We also note that the tTIS field strengths achieved according to

565   our simulations (in the range of 0.5-0.6 V/m) were sufficient to induce behavioral and neural

566   effects, in line with recent data[52,53] (see also [48]). Determining the minimum effective dose for tTIS

567   is an important line of future research given recent simulation results suggesting that stimulation

568   via an amplitude modulation with high frequency carrier signals (such as arising during tTIS) may

569   require higher dosages compared to conventional electrical stimulation with low frequencies (such

570   as during tACS), likely due to the low-pass filtering properties of neurons[43,105].

571   Finally, the strength of the behavioural effects of tTIS can be considered small to medium[106]

572   (d=0.2-0.5). We note that these effect sizes are consistent with studies applying other types of

573   non-invasive brain stimulation in healthy young adults, both in the context of motor learning (see

574   [107] for a meta-analysis), and reward tasks (e.g., [108,109]), despite the much longer stimulation time

575   used in these studies (between 3 and 20 times longer). Overall, albeit moderate, we believe that

576   the present effect sizes are relevant and consistent with what can be expected from the non-

577   invasive brain stimulation literature.

578

Limitations

580   The present study includes some limitations that we would like to acknowledge. First, at

581   the imaging level, we did not find a significant effect of reinforcement at the whole-brain level. This

582   might be due to the short duration of the task (6x40s), combined with the fact that we did not

583   couple reinforcement to monetary incentives, a manipulation known to strongly boost striatal

584   activity in the context of motor learning[18]. Yet, when considering BOLD activity in the striatal ROIs,

585   we did find a significant effect of reinforcement, suggesting that our experimental manipulation did

586   increase striatal activity but that the strength of the effect was insufficient to survive at the whole-

587 brain level. Second, we did not find any effect of tTIS when considering averaged BOLD activity.

588 Again, the short duration of the blocks may contribute to this non-significant effect. Another

589 possible interpretation is that the effect of tTIS on BOLD activity is not uniform across participants

590 as it likely depends on individual anatomy and function of the targeted brain region, as observed

591 for other non-invasive brain stimulation techniques[110]. Consistently, we found a correlation

592 between levels of impulsivity and the neural effects of $tTIS_{80Hz}$ (both BOLD and connectivity, Figure

593 S7). Importantly though, when including learning as a behavioral regressor we did find significant

594 clusters of correlation specifically in the striatum (Figure 3), suggesting that the behavioural effects

595 were indeed related to modulation of activity in the target region. Notably, this result was significant

596 when contrasting $tTIS_{80Hz}$ to the active control ($tTIS_{20Hz}$), but not to $tTIS_{Sham}$. Overall, we believe

597 that the fMRI data does provide interesting support that the behavioural effects of the stimulation

598 were indeed related to modulation of neural activity in the striatum, also in line with the present

599 simulations on realistic head models (Figure 1) and the connectivity results (Figure 4). This idea

600 is also in agreement with another recent study investigating the effects of tTIS on motor sequence

601 learning[52]. Notably though, a limitation of the present dataset is the very short duration of

602 stimulation and imaging for each experimental condition, that may explain some inconsistencies

603 in the results. Hence, following this first proof-of-concept study showing robust behavioural effects

604 and related neural changes, future studies including longer fMRI and stimulation sessions are

605 required to further confirm these results.

606 Finally, within the present study the computational modelling was performed on a realistic,

607 detailed head model (i.e., the MIDA model[59], see Methods). One limitation of this approach is that

608 the electric field simulations do not take individual structural information into account. Such

609 individual modeling would require information on brain anisotropy, an aspect that is likely to

610 significantly influence tTIS exposure[44,111]. However, in the present study diffusion MRI to evaluate

611   fractional anisotropy was not acquired. Future studies including diffusion MRI data will allow for

612   personalised modelling, paving the way for individualised tTIS informed by brain structure[53].

613

614   **Conclusion**

615   The present findings show for the first time the ability of non-invasive striatal tTIS to

616   interfere with reinforcement learning in humans through a selective modulation of striatal activity

617   and support the causal functional role of the human striatum in reinforcement motor learning. This

618   deep brain stimulation was well tolerated and compatible with efficient blinding, suggesting that

619   tTIS provides the exciting option to circumvent the steep depth-focality trade-off of current non-

620   invasive brain stimulation approaches in a safe and effective way. Overall, tTIS opens new

621   possibilities for the study of causal brain-behaviour relationships and for the treatment of neuro-

622   psychiatric disorders associated to alterations of deep brain structures.

4. Methods

4.1. Participants

A total of 48 right-handed healthy volunteers participated in the study. 24 participants were enrolled for the main tTIS study (15 women, 25.3 ± 0.7 years old; mean ± SE). Another group of 24 volunteers participated in the behavioural control experiment (Figure S2, 14 women, 24.2 ± 0.5 years old). Handedness was determined via a shortened version of the Edinburgh Handedness inventory[112] (laterality index = 89.3 ± 2.14% for the main study and 86.4 ± 2.51% for the control experiment). None of the participants suffered from any neurological or psychiatric disorder, nor taking any centrally-acting medication (see Supplementary Materials for a complete list of exclusion criteria). All participants gave their written informed consent in accordance with the Declaration of Helsinki and the Cantonal Ethics Committee Vaud, Switzerland (project number 2020-00127). Finally, all participants were asked to fill out a delay-discounting monetary choice questionnaire[113], which evaluates the propensity of subjects to choose smaller sooner rewards over larger later rewards, a preference commonly associated to choice impulsivity[75,114].

4.2. Experimental procedures

The study employed a randomised, double-blind, sham-controlled design. Following screening and inclusion, participants were invited to a single experimental session including performance of a motor learning task with concurrent transcranial electric Temporal Interference stimulation (tTIS) of the striatum and functional magnetic resonance imaging (fMRI). Overall, participants practiced 6 blocks of trials, that resulted from the combination of two reinforcement feedback conditions ($Reinf_{TYPE}$: $Reinf_{ON}$ or $Reinf_{OFF}$) with three types of striatal stimulation ($tTIS_{TYPE}$: $tTIS_{Sham}$, $tTIS_{20Hz}$ or $tTIS_{80Hz}$).

648

649   4.2.1. Motor learning task

650

651   4.2.1.1. General aspects

652

653   Participants practiced an adaptation of a widely used force-tracking motor task[54,55] with a

654   fMRI-compatible fiber optic grip force sensor (Current designs, Inc., Philadelphia, PA, USA)

655   positioned in their right hand. The task was developed on Matlab 2018 (the Mathworks, Natick,

656   Massachusetts, USA) exploiting the Psychophysics Toolbox extensions[115,116] and was displayed

657   on a computer screen with a refresh rate of 60 Hz. The task required participants to squeeze the

658   force sensor to control a cursor displayed on the screen. Increasing the exerted force resulted in

659   the cursor moving vertically and upward in a linear way. Each trial started with a preparatory period

660   in which a sidebar appeared at the bottom of the screen (**Figure 1A**). After a variable time interval

661   (0.9 to 1.1 s), a cursor (black circle) popped up in the sidebar and simultaneously a target (grey

662   larger circle with a cross in the middle) appeared, indicating the start of the movement period.

663   Subjects were asked to modulate the force applied on the transducer to keep the cursor as close

664   as possible to the center of the target. The target moved in a sequential way along a single vertical

665   axis for 7 s. The maximum force required (i.e., the force required to reach the target when it was

666   in the uppermost part of the screen; $MaxTarget_{Force}$) was set at 4% of maximum voluntary

667   contraction (MVC) evaluated at the beginning of the experiment. This low force level was chosen

668   based on pilot experiments to limit muscular fatigue. Finally, each trial ended with a blank screen

669   displayed for 2 s before the beginning of the next trial.

670

671   4.2.1.2. Trial types and reinforcement manipulation

672

673   During the experiment, participants were exposed to different types of trials (**Figure 1A,**

674   **Video S1**). In Test trials, the cursor remained on the screen and the target was consistently

675   displayed in grey for the whole duration of the trial. These trials served to evaluate Pre- and Post-

676   training performance for each block, without any disturbance. In Reinf$_{ON}$ and Reinf$_{OFF}$ trials (used

677   during Training only), we provided only partial visual feedback to the participants in order to

678   increase the impact of reinforcement on learning[4,56–58]. As such, the cursor was only intermittently

679   displayed during the trial: it was always displayed in the first second of the trial, and then

680   disappeared for a total of 4.5 s randomly split on the remaining time by bits of 0.5 s. The cursor

681   was therefore displayed 35.7% of the time during these trials (2.5 s over the 7 s trial). Importantly,

682   contrary to the cursor, the target always remained on the screen for the whole trial and participants

683   were instructed to continue to track the target even when the cursor was away.

684   In addition to this visual manipulation, in Reinf$_{ON}$ trials, participants also trained with

685   reinforcement feedback indicating success or failure of the tracking in real time. As such,

686   participants were informed that, during these trials, the color of the target would vary as a function

687   of their performance: the target was displayed in green when tracking was considered as

688   successful and in red when it was considered as failure. Online success on the task was

689   determined based on the Error, defined as the absolute force difference between the force

690   required to be in the center of the target and the exerted force[4,54–56]. The Error, expressed in

691   percentage of MVC, was computed for each frame refresh and allowed to classify a sample as

692   successful or not based on a closed-loop reinforcement schedule[8]. More specifically, for each

693   training trial, a force sample (recorded at 60 Hz, corresponding to the refresh rate of the monitor)

694   was considered as successful if the computed Error was below the median Error over the 4

695   previous trials at this specific sample. Put differently, to be successful, participants had to

696   constantly beat their previous performance. This closed-loop reinforcement schedule allowed us

697   to deliver consistent reinforcement feedback across individuals and conditions (see control

32

698   analysis on success rates in the Supplementary materials), while maximizing uncertainty on the

699   presence of reinforcement, an aspect that is crucial for efficient reinforcement motor learning[117].

700   Notably, in addition to this closed-loop design, samples were also considered as successful if the

701   cursor was very close to the center of the target (i.e., within one radius around the center,

702   corresponding to an Error below 0.2% of MVC). This was done to prevent any conflict between

703   visual information (provided by the position of the cursor relative to the target) and reinforcement

704   feedback (provided by the color of the target), which could occur in situations of extremely good

705   performance (when the closed-loop Error cut-off is below 0.2% of MVC).

706   As a control, $Reinf_{OFF}$ trials were similar to $Reinf_{ON}$ trials with the only difference that the

707   displayed colors were either cyan or magenta, and were generated randomly. Participants were

708   explicitly told that, in this condition, colors were displayed randomly and could be ignored. The

709   visual properties of the target in the $Reinf_{OFF}$ condition were designed to match the $Reinf_{ON}$

710   condition in terms of relative luminance (cyan: RGB = [127.5 242.1 255] matched to green: [127.5

711   255 127.5] and magenta: [211.7 127.5 255] to red: [255 127.5 127.5]) and average frequency of

712   change in colors (i.e., the average number of changes in colors divided by the total duration of a

713   trial, see Supplementary materials).

714   Notably, in this task, Training trials differed from Test trials regarding not only the color of

715   the target (red/green or cyan/magenta in Training trials and grey in Test trials) but also the visual

716   feedback experienced (partial and full visual feedback in Training and Test trials, respectively).

717   This choice was motivated by several reasons. First, we wanted to evaluate learning in the

718   classical, unperturbed, version of the force-tracking task[54,55], which is compatible with clinical

719   translation. Second, based on additional behavioural data on another group of participants (n =

720   24, see Figure S2), we found that significant effects of reinforcement on learning were observed

721   only when training was performed with partial visual feedback (displayed on 35.7% of the trial

722   time, as in the present study), in line with previous results[57,62]. However, this additional study also

33

723 revealed very limited improvement of performance during training with partial visual feedback,

724 potentially due to ceiling effects on performance in this condition. Yet, the improvement of

725 performance when comparing the Pre and Post-training assessments strongly suggested that

726 practicing the task with partial visual feedback still induced significant learning of the skill. Finally,

727 the change in visual feedback between Training and Post-training was the same in all

728 experimental conditions; this aspect of the task is therefore unlikely to explain the reinforcement

729 as well as the stimulation effects reported here.

730 Even though our study focused on reinforcement motor learning, it is worth mentioning that

731 other learning mechanisms such as error-based or strategic processes are likely to be also

732 engaged during the force-tracking task and may have recruited other brain regions beyond the

733 striatum (Spampinato and Celnik, 2020). Notably though, our protocol was specifically designed

734 to compare in the same individuals, learning in $Reinf_{ON}$ and $Reinf_{OFF}$ conditions while keeping the

735 other parameters of the task constant, to specifically isolate the contribution of reinforcement

736 processes in motor learning.

737

738 4.2.1.3. Motor learning protocol

739

740 After receiving standardised instructions about the force-tracking task, participants

741 practiced 5 blocks of familiarization (total of 75 trials) without tTIS. The first block of familiarization

742 included 20 trials with the target moving in a regular fashion (0.5 Hz sinuoid). Then, in a second

743 block of familiarization, participants performed 35 trials of practice with an irregular pattern, with

744 the same properties as the training patterns (see below). Finally, we introduced the reinforcement

745 manipulation and let participants perform 2 short blocks (8 trials each) including $Reinf_{ON}$ and

746 $Reinf_{OFF}$ trials. These four first blocks of familiarization were performed outside the MRI

747 environment. A last familiarization block (4 trials) was performed after installation in the scanner,

34

748   to allow participants to get used to performing the task in the MRI. This long familiarization allowed

749   participants to get acquainted with the use of the force sensor, before the beginning of the

750   experiment.

751   During the main part of the experiment, participants performed 6 blocks of trials in the MRI

752   with concurrent striatal tTIS (**Figure 1B**). Each block was composed of 4 Pre-training trials

753   followed by 24 Training and 8 Post-training trials. Pre- and Post-training trials were performed in

754   Test conditions, without tTIS and were used to evaluate motor learning. Training trials were

755   performed with or without reinforcement feedback and with concomitant striatal tTIS and were

756   used as a proxy of motor performance. During Training, trials were interspersed with 25 s resting

757   periods every 4 trials (used for fMRI contrasts, see below). The order of the 6 experimental

758   conditions was pseudo-randomised across participants: the 6 blocks were divided into 3 pairs of

759   blocks with the same tTIS condition and each pair was then composed of one $Reinf_{ON}$ and one

760     $Reinf_{OFF}$ block. Within this structure, the order of the $tTIS_{TYPE}$ and $Reinf_{TYPE}$ conditions were

761   balanced among the 24 participants. Hence, this randomisation allowed us to ensure that any

762   order effect that may arise from the repetition of the learning blocks would have the same impact

763   on each experimental condition (e.g., 4 subjects experienced $tTIS_{80Hz}$ - $Reinf_{ON}$ in the first block, 4

764   other subjects in the second block, 4 in the third block etc.).

765   As mentioned above, the protocol involved multiple evaluations of motor learning within

766   the same experimental session. In order to limit carry-over effects from one block to the following,

767   each experimental block was associated to a different pattern of movement of the target (**Figure**

768   **S1**). Put differently, in each block, participants had to generate a new pattern of force to

769   successfully track the target. To balance the patterns' difficulty, they all consisted in the summation

770   of 5 sinusoids of variable frequency (range: 0.1-1.5 Hz) that presented the following properties: a)

771   Average force comprised between 45 and 55% of the $MaxTarget_{Force}$; b) Absolute average

772   derivative comprised between 54 and 66 % of the $MaxTarget_{Force}$/s; c) Number of peaks = 14

773   (defined as an absolute change of force of at least 1% of $MaxTarget_{Force}$). These parameters were

774   determined based on pilot experiments to obtain a relevant level of difficulty for young healthy

775   adults and consistent learning across the different patterns.

776

777   4.2.2. Transcranial Electric Temporal Interference Stimulation (tTIS) applied to the
778   striatum

779

780   4.2.2.1. General concept

781

782   Transcranial temporal interference stimulation (tTIS) is an innovative non-invasive brain

783   stimulation approach, in which two or more independent stimulation channels deliver high-

784   frequency currents in the kHz range (oscillating at f1 and f1 + Δf; **Figure 1C**). These high-

785   frequency currents are assumed to be too high to effectively modulate neuronal activity [41,50,118].

786   Still, by applying a small shift in frequency, they result in a modulated electric field with the

787   envelope oscillating at the low-frequency Δf (target frequency) where the two currents overlap.

788   The peak of the modulated envelope amplitude can be steered towards specific areas located

789   deep in the brain, by tuning the position of the electrodes and current ratio across stimulation

790   channels[41] (**Figure 1C, 1D**). Based on these properties, tTIS has been shown to be able to focally

791   target activity of deep structures in rodents, without engaging overlying tissues[41]. Here, we applied

792   temporal interference stimulation transcranially via surface electrodes applying a low-intensity,

793   sub-threshold protocol following the currently accepted cut-offs and safety guidelines for low-

794   intensity transcranial electric stimulation in humans[119].

795

796   4.2.2.2. Stimulators

797

36

798　　　　The currents for tTIS were delivered by two independent DS5 isolated bipolar constant

799　　current stimulators *(Digitimer Ltd, Welwyn Garden City, UK)*. The stimulation patterns were

800　　generated using a custom-based Matlab graphical user interface and transmitted to the current

801　　sources using a standard digital-analog converter *(DAQ USB-6216, National Instruments, Austin,*

802　　*TX, USA)*. Finally, an audio transformer was added between stimulators and subjects, in order to

803　　avoid possible direct current accumulation.

804

805　　　　　　4.2.2.3. Stimulation protocols

806

807　　　　During the 6 Training blocks, we applied three different types of striatal tTIS (2 blocks

808　　each): a stimulation with a tTIS envelope modulated at 20Hz (tTIS$_{20Hz}$), a stimulation with a tTIS

809　　envelope modulated at 80Hz (tTIS$_{80Hz}$) and a sham stimulation (tTIS$_{Sham}$). For tTIS$_{20Hz}$, the

810　　posterior stimulation channel (TP7-TP8, see below) delivered a 1.99 kHz stimulation while the

811　　anterior one delivered a 2.01 kHz (Δf = 20 Hz). For tTIS$_{80Hz}$, the posterior and anterior channels

812　　delivered 1.96 kHz and 2.04 kHz, respectively (Δf = 80 Hz). Hence in both conditions, the high

813　　frequency component was comparable and the only difference was Δf. During each block, tTIS

814　　was applied for 5 minutes (6 x 50 s) during Training. Each stimulation period started and ended

815　　with currents ramping-up and -down, respectively, for 5 s. tTIS was applied only while participants

816　　were performing the motor task and not during resting periods or Pre- and Post-training

817　　assessments. Finally, tTIS$_{Sham}$ consisted in a ramping-up (5 s) immediately followed by a ramping-

818　　down (5 s) of 2 kHz currents delivered without any shift in frequency. This condition allowed us to

819　　mimic the sensations experienced during the active conditions tTIS$_{20Hz}$ and tTIS$_{80Hz}$, while

820　　delivering minimal brain stimulation (Figure S5). A trigger was sent 5 seconds before the beginning

821　　of each trial in order to align the beginning of the task and the beginning of the frequency shift

822　　after the ramp-up. Other tTIS parameters were set as follows: current intensity per stimulation

823   channel = 2 mA (baseline-to-peak), electrode type: round, conductive rubber with conductive

824   cream/paste, electrode size = 3 cm^2 (see ContES checklist in Supplementary materials for more

825   details).

826   The stimulation was applied within the MRI environment (Siemens 3T MAGNETOM

827   Prisma; Siemens Healthcare, Erlangen, Germany) using a standard RF filter module and MRI-

828   compatible cables *(neuroConn GmbH, Ilmenau, Germany)*. The technological, safety and noise

829   tests, and methodological factors can be found in Supplementary materials (Table S1) and are

830   based on the ContES Checklist [120].

831

832   4.2.2.4. Modelling

833

834   Electromagnetic simulations were carried out to identify optimised electrode placement

835   and current steering parameters. Simulations were performed using the MIDA head model[59], a

836   detailed anatomical head model featuring >100 distinguished tissues and regions that was derived

837   from multi-modal image data of a healthy female volunteer. Importantly, for brain stimulation

838   modelling, the model differentiates different scalp layers, skull layers, grey and white matter,

839   cerebrospinal fluid, and the dura and accounts for electrical conductivity anisotropy and neural

840   orientation based on diffusion tensor imaging (DTI) data. Circular electrodes (radius = 0.7 cm)

841   were positioned on the skin according to the 10-10 system and the electromagnetic exposure was

842   computed using the ohmic-current-dominated electro-quasistatic solver from Sim4Life v5.0 (ZMT

843   Zurich MedTech AG, Switzerland), which is suitable due to the dominance of ohmic currents over

844   displacement currents and the long wavelength compared with the simulation domain[121]. Dielectric

845   properties were assigned based on the IT'IS Tissue Properties Database v4.0[122]. Rectilinear

846   discretization was performed, and grid convergence as well as solver convergence analyses were

847   used to ensure negligible numerical uncertainty, resulting in a grid that included more than 54M

848   voxels. Dirichlet voltage boundary conditions, and then current normalization were applied. The

849   electrode-head interface contact was treated as ideal. tTIS exposure was quantified according to

850   the maximum modulation envelope magnitude formula from Grossman et al., (2017)[41]. Then, a

851   sweep over 960 permutations of the four electrode positions was performed, considering

852   symmetric and asymmetric montages with parallel (sagittal and coronal) or crossing current paths,

853   while quantifying bilateral striatum (putamen [BNA regions 225, 226, 229, 230], caudate [BNA

854   regions 219, 220, 227, 228] and nucleus accumbens [BNA regions 223, 224]) exposure

855   performance according to three metrics: a) target exposure strength, b) focality ratio (the ratio of

856   target tissue volume above threshold compared to the whole-brain tissue volume above threshold,

857   a measure of stimulation selectivity), and c) activation ratio (percentage of target volume above

858   threshold with respect to the total target volume, a measure of target coverage). We defined the

859   threshold as the 98th volumetric iso-percentile level of the tTIS. From the resulting Pareto-optimal

860   front, two configurations stood out particularly: one that maximised focality and activation (AF3 -

861   AF4, P7 - P8) and a second one that accepts a reduction of these two metrics by a quarter, while

862   increasing the target exposure strength by more than 50% (F3-F4, TP7-TP8). This last montage

863   was selected, to ensure sufficient tTIS exposure in the striatum[52] (Figure 1C, 1D).

864

865   4.2.2.5. Electrode positioning and evaluation of stimulation-associated sensations

866

867   Based on the modelling approach described above, we defined the stimulation electrode

868   positions in the framework of the EEG 10-10 system[123]. The optimal montage leading in terms of

869   target (i.e. the bilateral striatum) exposure strength and selectivity, was composed of the following

870   electrodes: F3, F4, TP7 and TP8. Their locations were marked with a pen on the scalp and, after

871   skin preparation (cleaned with alcohol), round conductive rubber electrodes of 3 cm^2 were placed

872   adding a conductive paste (*Ten20, Weaver and Company, Aurora, CO, USA or Abralyt HiCl,*

873   *Easycap GmbH, Woerthsee-Etterschlag, Germany*) as an interface to the skin. Electrodes were

874   held in position with tape and cables were oriented towards the top in order to allow good

875   positioning inside the scanner. Impedances were checked and optimised until they were below 20

876   kΩ [48]. Once good contact was obtained, we tested different intensities of stimulation for each

877   stimulation protocol in order to familiarise the participants with the perceived sensations and to

878   systematically document them. $tTIS_{Sham}$, $tTIS_{20Hz}$ and $tTIS_{80Hz}$ were applied for 20 seconds with the

879   following increasing current amplitudes per channel: 0.5 mA, 1 mA, 1.5 mA and 2 mA. Participants

880   were asked to report any kind of sensation and, if a sensation was felt, they were asked to grade

881   the intensity from 1 to 3 (light to strong) as well as give at least one adjective to describe it (Figure

882   S5). Following this step, cables were removed to be replaced by MRI-compatible cables and a

883   bandage was added to apply pressure on the electrodes and keep them in place. An impedance

884   check was repeated in the MRI right before the training and then again at the end of all recordings.

885

886   4.2.3.   MRI data acquisition

887

888   Structural and functional images were acquired using a 3T MAGNETOM PRISMA scanner

889   (*Siemens, Erlangen, Germany*). T1-weighted images were acquired via the 3D MPRAGE

890   sequence with the following parameters: TR = 2.3 s; TE = 2.96 ms; flip angle = 9°; slices = 192;

891   voxel size = 1 × 1 × 1 mm, FOV = 256 mm. Anatomical T2 images were also acquired with the

892   following parameters: TR = 3 s; TE = 409 ms; flip angle = 120°; slices = 208; voxel size = 0.8 ×

893   0.8 × 0.8 mm, FOV = 320 mm. Finally, functional images were recorded using Echo-Planar

894   Imaging (EPI) sequences with the following parameters: TR = 1.25 s; TE = 32 ms; flip angle =

895   58°; slices = 75; voxel size = 2 × 2 × 2 mm; FOV = 112 mm.

896

897   **4.3.   Data and statistical analyses**

898

899   Data and statistical analyses were carried out with Matlab 2018a (the Mathworks, Natick,

900   Massachusetts, USA) and the R software environment for statistical computing and graphics (R

901   Core Team 2021, Vienna, Austria). Robust linear regressions were fitted with the Matlab function

902   robustfit. Linear mixed models (LMM) were fitted using the lmer function of the lme4 package in R

903   [124]. As random effects, we added intercepts for participants and block. Normality of residuals, and

904   homoscedasticity of the data were systematically checked, and logarithmic transformations were

905   applied when necessary (i.e., when skewness of the residuals' distribution was not comprised

906   between - 2 and 2[125] or when homoscedasticity was violated based on visual inspection). To

907   mitigate the impact of isolated influential data points on the outcome of the final model, we used

908   tools of the influence.ME package to detect and remove influential cases based on the following

909   criterion: distance > 4 * mean distance[126]. Statistical significance was determined using the anova

910   function with Satterthwaite's approximations of the lmerTest package[127]. For specific post-hoc

911   comparisons we conducted pairwise comparisons by computing estimated marginal means with

912   the emmeans package with Tukey adjustment of p-values[128]. Standardised effect size measures

913   were obtained using the eff_size function of the emmeans package[129]. The level of significance

914   was set at p<0.05.

915

916

917   4.3.1. Behavioural data

918

919   4.3.1.1. Evaluation of motor learning

920

921   The main goal of the present study was to evaluate the influence of striatal tTIS on

922   reinforcement motor learning. To do so, we first removed trials, in which participants did not react

923   within 1 s after the appearance of the cursor and target, considering that these extremely long

924   preparation times may reflect significant fluctuations in attention[130]. This occurred extremely rarely

925   (0.52 % of the whole data set). For each subject and each trial, we then quantified the tracking

926 Error as the absolute force difference between the applied and required force as done

927 previously[4,54,56]. Tracking performance during Training and Post-training trials were then

928 normalised according to subjects' initial level by expressing the Error data in percentage of the

929 average Pre-training Error for each block. In order to test our main hypothesis predicting specific

930 effects of striatal tTIS on reinforcement motor learning, we performed a LMM on the Post-training

931 data with $tTIS_{TYPE}$ and $Reinf_{TYPE}$ as fixed effects. We then also ran the same analysis on the

932 Training data, to evaluate if striatal tTIS also impacted on motor performance, while stimulation

933 was being delivered.

934 As a control, we checked that initial performance at Pre-training was not different between

935 conditions with a LMM on the Error data obtained at Pre-training. Again, $tTIS_{TYPE}$ and $Reinf_{TYPE}$

936 were considered as fixed effects. Finally, another LMM was fitted with the fixed effect $tTIS_{TYPE}$ to

937 verify that the amount of positive reinforcement (as indicated by a green target) in the $Reinf_{ON}$

938 blocks was similar across $tTIS_{TYPES}$.

939

940 4.3.2. fMRI data

941

942 4.3.2.1. Imaging Preprocessing

943

944 We analyzed functional imaging data using Statistical Parametric Mapping 12 (*SPM12;*

945 *The Wellcome Department of Cognitive Neurology, London, UK*) implemented in MATLAB

946 R2018a (*Mathworks, Sherborn, MA*). All functional images underwent a common preprocessing

947 including the following steps: slice time correction, spatial realignment to the first image,

948 normalization to the standard MNI space and smoothing with a 6 mm full-width half-maximal

949 Gaussian kernel. T1 anatomical images were then co-registered to the mean functional image and

950 segmented. This allowed to obtain bias-corrected gray and white matter images, by normalizing

951 the functional images via the forward deformation field. To select subjects with acceptable level of

952 head movement, framewise displacement was calculated for each run. A visual check of both non-

953   normalised and normalised images was performed in order to ensure good preprocessing quality.

954   Finally, possible tTIS-related artifacts were investigated based on signal to noise ratio maps (see

955   below).

956

957   4.3.2.2. Signal to Noise Ratio

958

959   Total signal to noise ratio (tSNR) maps were computed to check the presence of possible

960   artifacts induced by the electrical stimulation. The values were calculated per each voxel by

961   dividing the mean of the voxel time series by its standard deviation. Spherical regions of interest

962   were then defined both underneath the tTIS electrodes and at 4 different locations, distant from

963   the electrodes as a control. The center of each spherical ROI was obtained by projecting the

964   standard MNI coordinates of each electrode on the scalp[131] toward the center of the brain. After

965   visual inspection of the ROIs, average tSNR maps were extracted within each sphere. A LMM was

966   used to compare the average SNR underneath the electrodes versus the control regions and

967   between stimulation protocols. The results of this analysis are presented in Supplementary

968   materials (Figure S8).

969

970   4.3.2.3. Task-based BOLD activity analysis

971

972   A general linear model was implemented at the single-subject level in order to estimate

973   signal amplitude. Eight regressors were included in the model: 6 head motion parameters

974   (displacement and rotation) and normalised time series within the white matter and the

975   corticospinal fluid. Linear contrasts were then computed to estimate specific activity during the

976   motor task with respect to resting periods. Functional activation was also extracted within specific

977   ROIs individually defined based on structural images. More specifically, the Freesurfer recon-all

978   function   was   run   based   on   the   structural   T1w   and   T2w   images

43

979   (https://surfer.nmr.mgh.harvard.edu/). The BNA parcellation was derived on the individual subject

980   space and the selected ROIs were then co-registered to the functional images and normalised to

981   the MNI space. BOLD activity within the individual striatal masks was averaged and compared

982   between different striatal nuclei namely the putamen (BNA regions 225, 226, 229, 230), caudate

983   (BNA regions 219, 220, 227, 228) and nucleus accumbens (BNA regions 223, 224). Comparison

984   between conditions were presented for uncorrected voxel-wise FWE, p=0.001 and multiple

985   comparison corrected at the cluster level to reduce False Discovery Rate (FDR), p=0.05.

986

987

988   4.3.2.4. Effective connectivity analyses

989

990   As an additional investigation, we computed task-modulated effective functional

991   connectivity by means of the CONN toolbox 2021a (www.nitrc.org/projects/conn,

992   RRID:SCR_009550) running in Matlab R2018a (*Mathworks, Sherborn, MA*). An additional

993   denoising step was added by applying a band-pass filtering from 0.01 to 0.1 Hz and by regressing

994   potential confounders (white matter, CSF and realignment parameters). After that, generalized

995   Psycho-Physiological Interactions (gPPI) connectivity was extracted within specific pre-defined

996   customised sub-networks: a reward and a motor network. gPPI evaluates condition-specific

997   changes in effective connectivity, defined as the directed effect that one brain region has on

998   another under some model of neuronal coupling (Friston, 1994). In particular, gPPI considers a

999   series of equations in which activity in a ROI (pre-defined frontal areas in our case) depends on a

1000   specific condition (the 'psychological' factor) and on activity in the seed region (striatum here, the

1001   'physiological' factor). By solving these equations, it is possible to determine a coefficient that

1002   represents task-modulation of effective connectivity[132]. Importantly, task-related changes in

44

1003 effective connectivity are expressed relative to rest, and therefore values closer to 0 reflect a

1004 connectivity similar to resting state.

1005

1006   The reward network was defined as following: two regions within the striatum, namely the

1007 NAc (BNA regions 223 and 224) and the ventro-medial putamen (BNA regions 225 and 226, left

1008 and right respectively), and two frontal areas, namely the anterior cingulate (BNA regions 177,

1009 179, 183 and 178, 180, 184, left and right respectively) and the orbitofrontal cortex within the

1010 vmPFC (BNA regions 41, 45, 47, 49, 187 and 42, 46, 48, 50, 188 for left and right respectively).

1011 The motor network included the following areas: the dorso-lateral putamen (BNA 229, 230, for left

1012 and right respectively), the dorsal caudate (BNA regions 227, 228 for left and right respectively)

1013 the medial part of the SMA (BNA regions 9 and 10, left and right respectively) and the part of the

1014 M1 associated to upper limb function (BNA regions 57 and 58, left and right respectively). Notably,

1015 we considered connectivity in the left and right motor and reward networks regardless of laterality.

1016 These ROIs were selected based on the following rationale. First, they are consistent with previous

1017 literature on reinforcement learning of motor skills[68,90,133,134]. Second, there is structural and

1018 functional evidence for these fronto-striatal connections[135,136]. Third, the frontal areas included in

1019 the analyses are well-established hubs of the motor learning (M1 and SMA, see [12] for a meta-

1020 analysis) and reward networks (vmPFC and ACC, see [11] for a meta-analysis). Finally, gPPI was

1021 also extracted within a control language network, defined based on the functional atlas described

1022 by Shirer et al.(2012)[70].

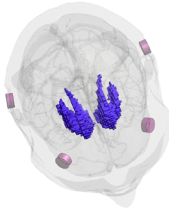**Supplementary material**

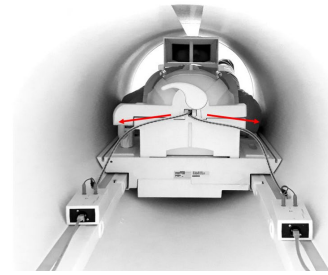**1. <u>Exclusion criteria</u>**

- Unable to consent
- Severe neuropsychiatric (e.g., major depression, severe dementia) or unstable systemic diseases (e.g., severe progressive and unstable cancer, life threatening infectious diseases)
- Severe sensory or cognitive impairment or musculoskeletal dysfunctions prohibiting to understand instructions or to perform the experimental tasks
- Color blindness
- Inability to follow or non-compliance with the procedures of the study
- Contraindications for NIBS or MRI:
  - Electronic or ferromagnetic medical implants/device, non-MRI compatible metal implant
  - History of seizures
  - Medication that significantly interacts with NIBS being benzodiazepines, tricyclic antidepressant and antipsychotics
- Regular use of narcotic drugs
- Left-handedness
- Pregnancy
- Request of not being informed in case of incidental findings
- Concomitant participation in another trial involving probing of neuronal plasticity.

1047   **2. ContES Checklist**

1048

Technological factors	
Manufacturer of Stimulator	DS5 Isolated Bipolar Constant Current Stimulator (Digitimer)
MR Conditional Electrode Details	Round, 3 cm2 conductive rubber electrodes
Electrode Positioning	F3 → F4 TP7 → TP8 A bandage is warped around the head to apply pressure and keep the electrodes in place Electrodes are oriented in order to have vertical cables entering parallel to the MRI coil Head was fixed with pillows to avoid movements
MR Conditional Skin-Electrode Interface	10-20 gel One or two drops of saline were added when impedances were too high
Amount of Contact Medium (Paste/Gel/Electrolyte)	Around 1mm of paste was manually placed on the electrodes
Electrode Placement Visualization	Pictures

|	
RF Filter	NeuroConn DC-STIMULATOR MR RF filter module with MRI-compatible cables and electrodes
Wire Routing Pattern	10 m ethernet cables between inner and outer box pass through a conduit along the wall of the MRI room until reaching the back of the MRI. Cables are then fixed with straps on the ground and on the wall of the MRI machine in order to avoid loops until reaching the interior of the coil. Cables between the head and the inner boxes were also fixed with straps and they were oriented in order to exit the magnetic field direction as soon as possible as indicated by the red arrows of the image below.
tES-fMRI Machine Synchronization/Communication	Stimulation was triggered by the stimulus delivery PC via parallel port to BNC cable. The parallel port of the stimulus delivery PC was connected to the DAQ controlling the stimulators. Stimulus delivery PC, in turn, was also receiving the scanner trigger from the scanner via USB port.
Safety and noise tests	
MR Conditionality Specifics for tES Setting	Please refer to Section "Methods-Imaging acquisition"
tES-fMRI Setting Test - Safety Testing	Impedances were checked before and after

	the stimulation. No temperature tests were performed during the experiment. Intensity titration was performed prior to entering the MRI, testing increasing currents (0.5, 1, 1.5 and 2 mA) and asking the subject to report any type of sensation. A sensation questionnaire was also performed at the end of the experiment.
tES-fMRI Setting Test - Subjective Intolerance Reporting	No intolerances were reported by any subject
tES-fMRI Setting Test - Noise/Artifact	Signal to Noise Ratio (SNR) analysis was performed on the fMRI images, please refer to Section "Methods-Signal to Noise Ratio"
Impedance Testing	Impedances were checked right after electrodes positioning outside the scanner, before and after the stimulation inside. One or two drops of saline solution were added if impedances were higher than 20kΩ
Methodological factors	
Concurrent tES-fMRI Timing	For timings, please refer to the "Methods-Stimulation protocols" section To mitigate the impact of potential carry-over effects on our experimental results we used the following strategy: 1) We stimulated for short periods in each condition (5 minutes interspersed with resting periods without stimulation; see "Methods-Stimulation protocols"); 2) We imposed breaks (~7-8 minutes) between each stimulation protocol; 3) We randomised the order of the

	Stimulation conditions
Imaging Session Timing	All sequences were performed with TI stimulation electrodes placed on the subjects' head.
tES Experience Report	Please refer to "Results" section and to Figure S5.

Table S1. ContES checklist as recommended in Ekhtiari et al., 2022[120] for concurrent tES-fMRI studies.

3. Patterns of motion of the target used in the study
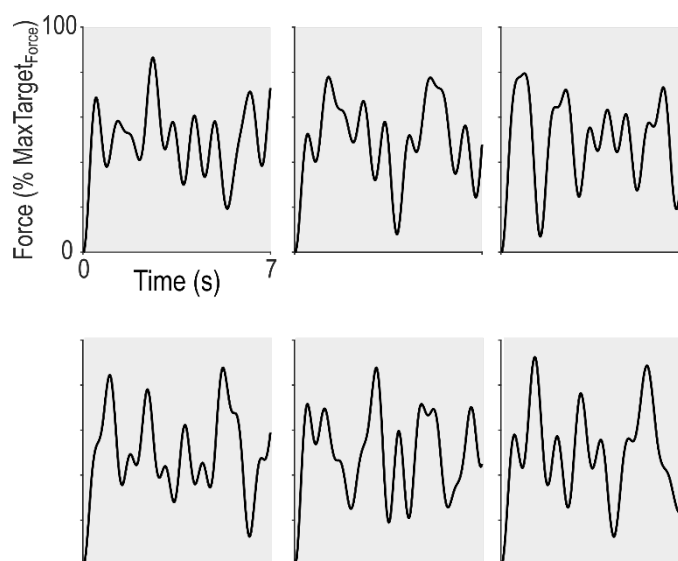
Figure S1. Patterns of motion of the target. For each block of training, participants had to learn a new pattern of motion of the target. The patterns had similar mathematical properties and their relationship to a condition was randomised (see Methods for more details).
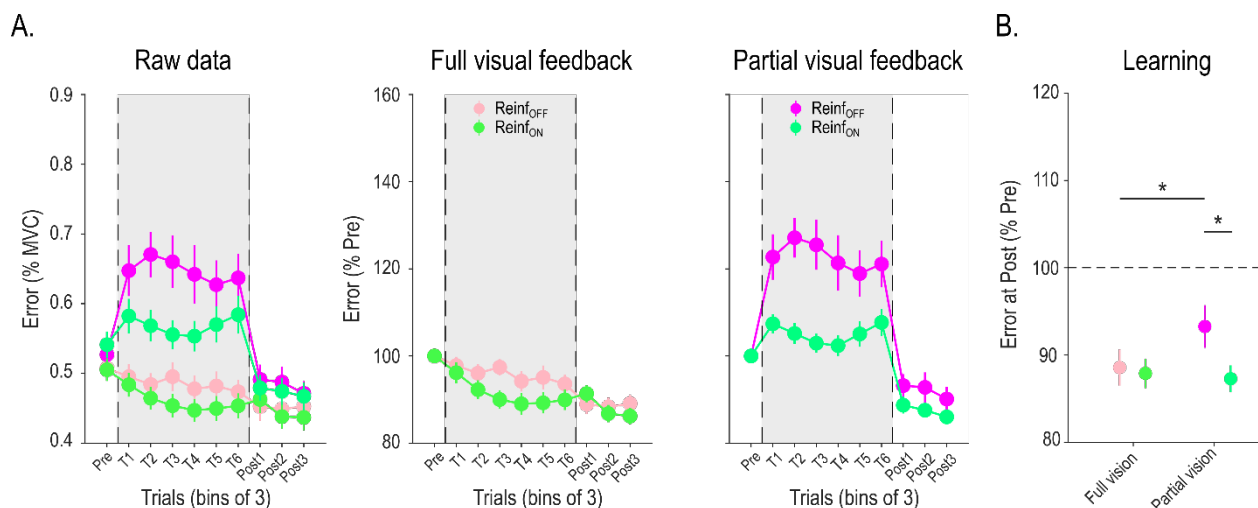
4. Additional behavioural experiment

To determine the optimal experimental parameters to study reinforcement learning of motor skills, we performed an additional behavioural experiment, in the absence of brain stimulation and imaging. In particular, we tested the relationship between the amount of visual feedback available during Training and the benefits of reinforcement in the force-tracking task. Another group of young healthy participants (n=24; 14 women, 24.2 ± 0.5 years old, independent

1065   from the subjects tested in the main experiment) performed blocks of the task with $Reinf_{ON}$ or

1066 $Reinf_{OFF}$ and with either full visual feedback or only partial visual feedback (cursor displayed for

1067   35.7% of the total trial duration, as in the main study). Each learning block was composed of 30

1068   trials (vs. 36 trials in the main study) and in addition to real-time closed-loop reinforcement

1069   feedback, participants also received endpoint feedback on their overall performance after each

1070   trial during Training (i.e., indicating success or failure on the trial). The LMM ran on the Post-

1071   training data revealed a significant effect of visual feedback ($F_{(1,788.33)}$=5.90; p=0.015),

1072   reinforcement ($F_{(1,787.87)}$=11.64; p<0.001) and a significant interaction between these two factors

1073   ($F_{(1,788.03)}$=10.27; p=0.0014, **Figure S2A**). Interestingly, Tukey-corrected post-hoc tests showed

1074   that the interaction was due to the fact that while reinforcement did not improve learning when

1075   Training was performed with full visual feedback (p=0.88, d=0.014), it induced robust benefits

1076   when training with partial visual feedback (p<0.001, d=0.46, **Figure S2B**). This result is in line with

1077   previous literature showing that reinforcement feedback is particularly beneficial for motor learning

1078   when visual feedback is uncertain[57,62]. Based on the outcome of this additional study, we decided

1079   to train participants with partial visual feedback in the present experiment to evaluate the effect of

1080   tTIS in a version of the task that yielded significant reinforcement gains. Notably, this work also

1081   shows that the effect of reinforcement on motor learning observed in the $tTIS_{Sham}$ and $tTIS_{20Hz}$

1082   conditions (Figure 2) is reproducible.

Figure S2. Results of an additional behavioural experiment (n = 24). A) Motor performance across training. Raw Error data (expressed in % of Maximum Voluntary Contraction [MVC]) are presented on the left panel for the different experimental conditions in bins of 3 trials. On the right, the two plots represent the Pre-training normalised Error in the Full visual feedback and Partial visual feedback blocks (i.e., cursor displayed 35.7% of the time, as in the main experiment). Note the strong gains in motor performance, especially with partial visual feedback but also the limited improvement of performance during training in this condition. B) Motor learning. Averaged Error at Post-training (normalised to Pre-training) in the different experimental conditions are shown, for the subjects included in the analysis (i.e., after outlier detection, n=23). Reduction of Error at Post-training reflects true improvement at tracking the target in Test conditions (in the absence of reinforcement or visual uncertainty). The LMM ran on these data revealed significant a significant effect of reinforcement feedback on learning when training with partial, but not full, visual feedback. *: p<0.05. Data are represented as mean ± SE.

5. Evolution of motor performance in the different conditions

The main analysis revealed a general effect of tTIS on motor performance during Training, irrespective of the presence of reinforcement. As a subsequent analysis, we also asked whether the evolution of performance during Training depended on type of striatal stimulation applied. We ran the same LMM as in the main study (see Results) but with the addition of a continuous fixed effect Trial, allowing us to evaluate whether the slope of performance change was different according to $tTIS_{TYPE}$. (Figure S3). Indeed, this analysis revealed a significant $tTIS_{TYPE}$ x Trial interaction ($F_{(2, 3399)}=4.46$; p=0.012) that was due to different slopes in the $tTIS_{Sham}$ compared to the $tTIS_{20Hz}$ (p=0.013) and $tTIS_{80Hz}$ (at the trend level, p=0.068) conditions. Evolution of performance in the $tTIS_{20Hz}$ and $tTIS_{80Hz}$ conditions was not different (p=0.81). Notably, this effect

1109 could not be explained by differences in initial performance (all p>0.21 when comparing

1110 intercepts). Moreover, the effect of tTIS on motor improvement during Training did also not depend

1111 on the presence of reinforcement ($Reinf_{TYPE}$, $tTIS_{TYPE}$ and Trial: $F_{(2, 3399)}=0.51$; $p=0.60$). Overall,

1112 this analysis shows that the detrimental effect of striatal tTIS on motor performance is due to an

1113 impaired ability to improve performance with practice and further confirms that tTIS did not

1114 modulate the ability to use reinforcement feedback during Training.
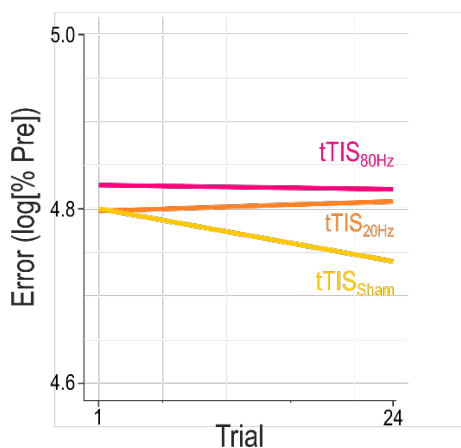
1115

Figure S3. Slopes of performance change during Training in the different stimulation conditions. Modeled performance change for $tTIS_{Sham}$, $tTIS_{20Hz}$ and $tTIS_{80Hz}$ throughout Training. The $tTIS_{TYPE}$ x Trial interaction revealed that performance improved more with $tTIS_{Sham}$ compared to $tTIS_{20Hz}$ and $tTIS_{80Hz}$. Notably this effect was not modulated by the presence of reinforcement and could not be explained by differences in intercepts.

1121

1122

1123 **6. Effect of visual and reinforcement feedback on motor performance**

1124

1125 As a control, we asked whether the tTIS and reinforcement effects reported in Figure 2

1126 depended on the availability of visual information during Training. To do so, we computed the

1127 normalised Error for phases with the $Cursor_{ON}$ or $Cursor_{OFF}$ (taking into account a lag of 0.25s,

1128 corresponding to the estimated visuo-motor delay in this type of task for young healthy subjects[137])

1129 and analysed these data in a LMM including the factors $Reinf_{TYPE}$, $tTIS_{TYPE}$ and $Cursor_{TYPE}$. As in

1130 the main analysis, we confirmed the effect of $Reinf_{TYPE}$ ($F_{(1, 6872)}=344.87$; $p<0.001$), $tTIS_{TYPE}$

1131 ($F_{(2,6872)}=28.79$; $p<0.001$) and the absence of interaction between these two factors ($F_{(2,6875.4)}=0.49$;

1132   p=0.61, Figure S4). This analysis also revealed a Cursor$_{TYPE}$ effect ($F_{(2,6875.3)}$=49.66; p<0.001)

1133   which was due to the fact that the Error was generally higher in the absence visual information on

1134   the position of the cursor (d=0.17). Interestingly, there was also a Reinf$_{TYPE}$ x Cursor$_{TYPE}$ interaction

1135   ($F_{(2,6872)}$=29.35; p<0.001): while benefits of reinforcement were significant in both the Cursor$_{ON}$

1136   (p<0.001, d=0.32) and Cursor$_{OFF}$ (p<0.001, d=0.58) conditions, the magnitude of the

1137   reinforcement-related gains in performance were larger in the Cursor$_{OFF}$ condition (t-test

1138   comparing the gains: $t_{(46)}$=2.74, p=0.0086). Moreover, post-hoc tests also revealed that the

1139   absence of vision of the cursor was detrimental for performance in the Reinf$_{OFF}$ condition (p<0.001,

1140   d=0.30) but not in presence of Reinf$_{ON}$ (p=0.25, d=0.039). Hence, the presence of reinforcement

1141   was particularly beneficial when visual information was not available, in line with previous

1142   research[57,62] and also in agreement with the results of our additional experiment (Figure S2).

1143   Importantly, the LMM did not reveal any interaction between tTIS$_{TYPE}$ and Cursor$_{TYPE}$ ($F_{(2,6872)}$=0.49;

1144   p=0.31) and no triple interaction ($F_{(2,6872)}$=1.53; p=0.22), confirming that striatal tTIS had a global

1145   effect on motor performance during Training, which did not depend on the presence of visual and

1146   reinforcement feedback.

1147
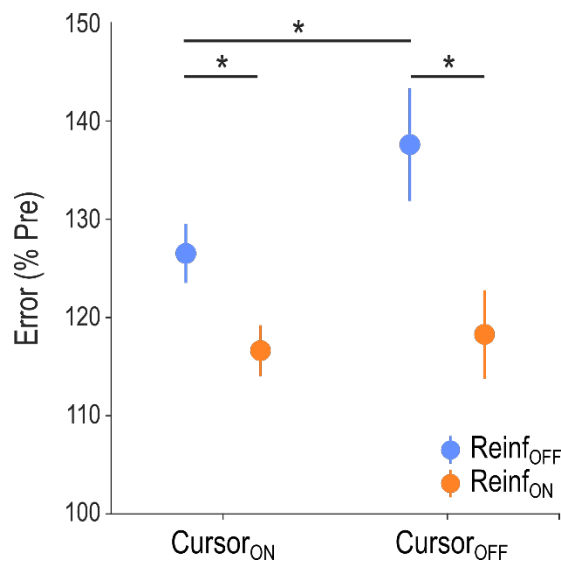
1149   **Figure S4. Effect of visual and reinforcement feedback on motor performance.** Pre-
1150   training normalised Error depending on the presence of the cursor (Cursor$_{ON}$ or Cursor$_{OFF}$), and

1151 the presence of reinforcement feedback during Training. The significant $Reinf_{TYPE}$ x $Cursor_{TYPE}$
1152 interaction was related to the fact that the benefits of reinforcement were stronger when visual
1153 information was not available. Notably, this analysis takes into account a visuo-motor delay of
1154 0.25s, as previously reported during a similar task (Lam and Zenon, 2021). *: p<0.05. Data are
1155 represented as mean ± SE.

1156

1157

1158 **7. <u>Control analyses of behavioural data</u>**

1159

1160 <u>Pre-training performance</u>

1161 In order to verify that our main behavioural results were not influenced by potential

1162 differences in initial performance between conditions despite randomisation, we analysed the

1163 Error at Pre-training between conditions. We did not find any $tTIS_{TYPE}$ ($F_{(2,519.15)}$=1.64; p=0.20) or

1164 $tTIS_{TYPE}$ x $Reinf_{TYPE}$ effect ($F_{(2,519.99)}$=1.08; p=0.34), suggesting that the main behavioural results

1165 could not be accounted for by differences in initial performance between conditions. However, the

1166 LMM did reveal a $Reinf_{TYPE}$ effect ($F_{(1,519.15)}$=12.47; p<0.001), that was due to the fact that Pre-

1167 training performance was generally better in $Reinf_{OFF}$ blocks. This effect, which was opposite to

1168 our learning results (generally better learning with $Reinf_{ON}$), may be related to an expectancy effect

1169 stemming from the repetitive structure of the reinforcement conditions (see Methods). However,

1170 the absence of interaction with $tTIS_{TYPE}$ is strongly suggestive that this effect did not drive any of

1171 the main findings. Put together, these data provide confidence that the differential effects of striatal

1172 tTIS on motor learning depending on the presence of reinforcement were not the result of different

1173 initial performance between conditions.

1174 <u>Success rate</u>

1175 Overall, the amount of positive reinforcement (i.e., when the target was green) averaged

1176 52.78 +/- 0.42% and was comparable across $tTIS_{TYPES}$ ($F_{(2,1702)}$=0.17; p=0.84), suggesting that the

1177 closed-loop reinforcement schedule was successful at providing similar reinforcement feedback

55

1178   despite differences in performance between conditions. Hence, different success rates during

1179   training cannot explain the effect of the different striatal tTIS conditions on motor learning.

1180   <u>Frequency of flashing</u>

1181   Analysis of the frequency of flashing in the different conditions did not reveal any effect of

1182 $tTIS_{TYPE}$ ($F_{(2,3283)}$=0.85; p=0.43) nor any $Reinf_{TYPE}$ x $tTIS_{TYPE}$ interaction ($F_{(2,3283)}$=0.19; p=0.82),

1183   suggesting that the behavioural effects of tTIS could not be explained by a visual confound.

1184   However, this analysis did reveal a $Reinf_{TYPE}$ effect ($F_{(1,3283)}$=33.62; p<0.001) which was due to the

1185   fact that the average frequency in the $Reinf_{OFF}$ condition (4.28 ± 0.097 Hz) was slightly but

1186   significantly higher than with $Reinf_{ON}$ (4.08 ± 0.098 Hz; $F_{(1,3283)}$=33.62; p<0.001). Notably, in

1187   absolute terms, this difference represented only a difference of 1.4 change of color over the whole

1188   7 s trial, which we think is unlikely to explain the improvement of performance in the $Reinf_{ON}$

1189   condition.

1190   <u>Order of the reinforcement conditions</u>

1191   Previous exposure to reinforcement feedback may improve subsequent learning through

1192   reinforcement[138]. Thanks to our randomisation procedure, the previous exposure to the $Reinf_{ON}$

1193   condition was equally counterbalanced in all stimulation conditions, and should therefore not

1194   influence our main results. Still, we performed an analysis to specifically investigate the effect of

1195   the previous exposure to $Reinf_{ON}$. To do so, we split the participants depending on whether they

1196   experienced $Reinf_{ON}$ or $Reinf_{OFF}$ first (12 subjects per group) and performed a new LMM on the

1197   Post-training data with the addition of a categorical factor $Group_{TYPE}$. In particular, if the previous

1198   exposure to the $Reinf_{ON}$ condition influenced following learning with reinforcement, we would

1199   expect to see a $Group_{TYPE}$ x $Reinf_{TYPE}$ interaction. The analysis did not indicate any $Group_{TYPE}$

1200   effect on learning ($F_{(1,21.96)}$=0.35; p=0.56), neither did it reveal a $Group_{TYPE}$ x $Reinf_{TYPE}$ ($F_{(1,4)}$=0.72;

1201   p=0.44), or a triple interaction with $tTIS_{TYPE}$ ($F_{(2,1105.06)}$=1.75; p=0.17). Overall, this analysis

1202   suggests that the order of the exposure to the reinforcement condition did not influence the present

1203   findings.

1204

8.   Blinding integrity and tTIS-evoked sensations
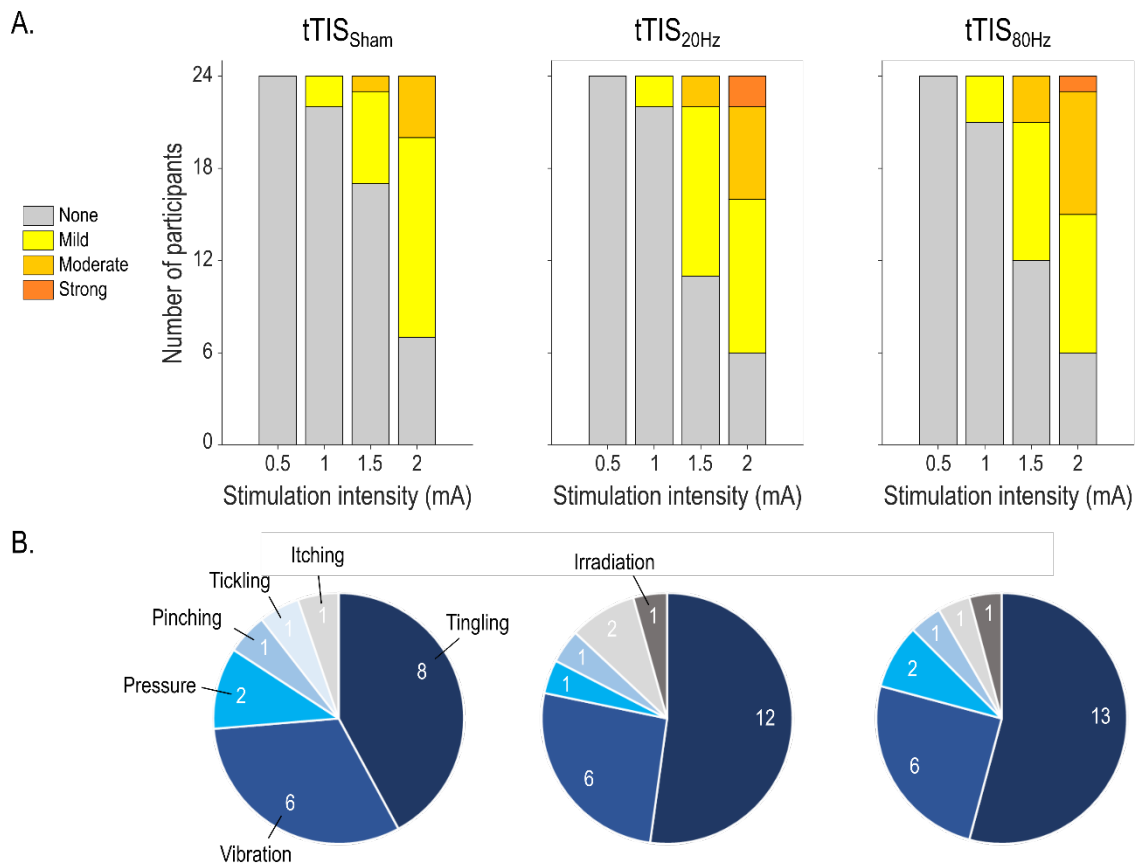
1206

Figure S5. tTIS-related sensations. A) Magnitude of tTIS-related sensations. Magnitude of sensations reported before the experiment for current amplitudes ranging from 0.5 to 2 mA for each $tTIS_{TYPE}$. The current amplitude used in the present experiment was 2 mA. **B) Types of tTIS-related sensations.** Type of sensations as described by the participants, at 2 mA. Note that subjects were allowed to describe their sensations with up to two different words.

1212

1213 ### 9. Brain activity during reinforcement motor learning
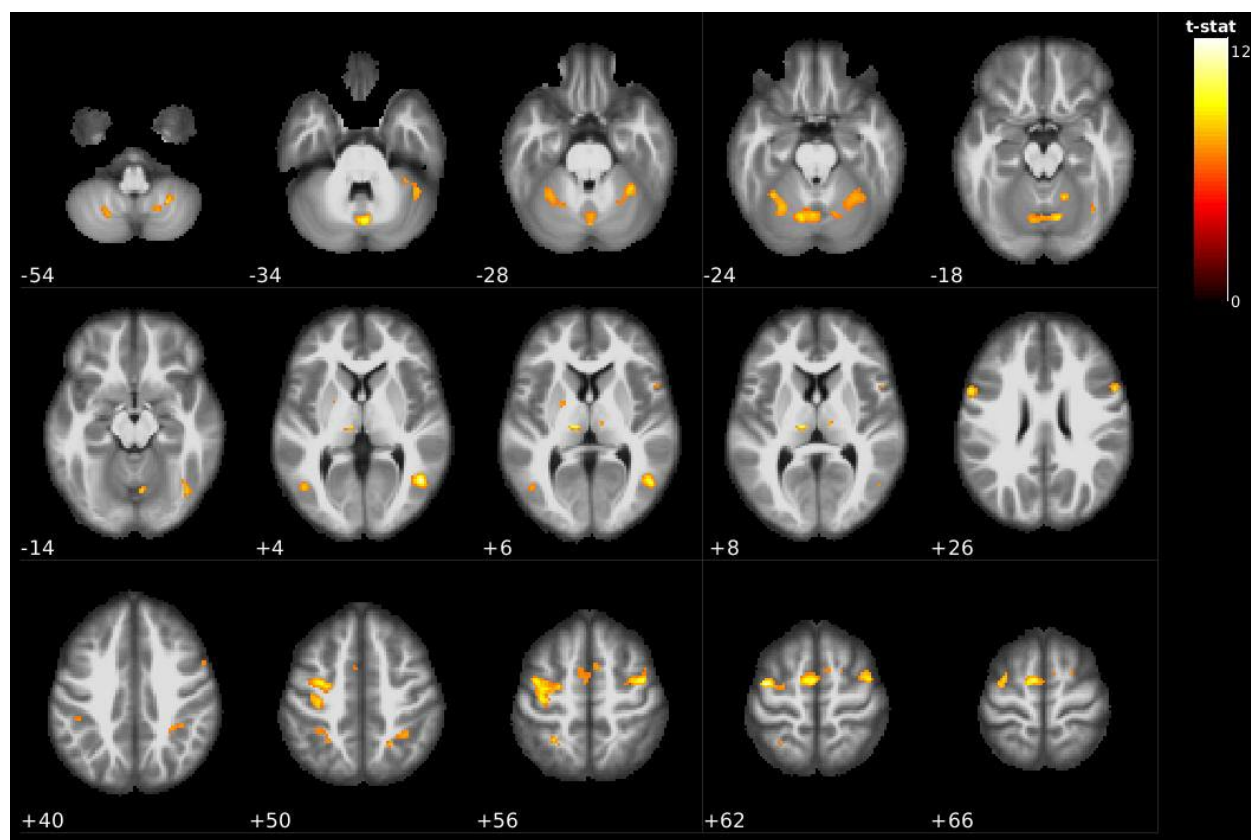
1214

1215 **Figure S6. Whole-brain activity during reinforcement motor learning.** Activation maps
1216 for the contrast task>rest in the tTIS$_{Sham}$, Reinf$_{ON}$ condition showing activation of key areas of the
1217 reinforcement motor learning network including the putamen, thalamus, cerebellum and
1218 sensorimotor network, especially on the left side. Significant clusters are shown for corrected
1219 voxel-wise family wise error (FWE), p=0.05, and corrected cluster-based false discovery rate
1220 (FDR), p=0.05.

1221
1222

Cluster-level				Peak-level					x	y	z	Region
$p_{FWE-corr}$	$q_{FDR-corr}$	k_E	P_{uncorr}	$p_{FWE-corr}$	$q_{FDR-corr}$	T	(Z_E)	P_{uncorr}				
<0.001	<0.001	135	<0.001	<0.001	0.005	12.63	6.84	<0.001	46	-62	4	Temporal_Mid_R
<0.001	<0.001	523	<0.001	<0.001	0.005	12.32	6.77	<0.001	-40	-8	62	Precentral_L
				<0.001	0.021	10.62	6.33	<0.001	-34	-6	52	Postcentral_L
				<0.001	0.021	10.43	6.28	<0.001	-36	-20	54	Precentral_L
<0.001	<0.001	335	<0.001	<0.001	0.018	11.08	6.46	<0.001	-8	-6	64	Supp_Motor_Area_L
				0.003	0.145	8.21	5.56	<0.001	6	6	58	Supp_Motor_Area_R
				0.003	0.145	8.20	5.55	<0.001	-4	-2	54	Supp_Motor_Area_L
<0.001	<0.001	44	<0.001	<0.001	0.021	10.65	6.34	<0.001	-10	-20	6	Thal_IL_L
<0.001	<0.001	162	<0.001	<0.001	0.021	10.36	6.26	<0.001	42	-6	56	Frontal_Mid_2_R
				<0.001	0.042	9.48	5.99	<0.001	34	-4	58	Frontal_Sup_2_R
<0.001	<0.001	175	<0.001	<0.001	0.021	10.27	6.23	<0.001	-58	10	28	Precentral_L
				<0.001	0.037	9.60	6.03	<0.001	-56	8	20	Frontal_Inf_Oper_L
				0.019	0.490	7.32	5.21	<0.001	-48	2	16	Rolandic_Oper_L
<0.001	<0.001	601	<0.001	<0.001	0.024	10.06	6.17	<0.001	2	-74	-34	Vermis_7
				<0.001	0.025	9.99	6.15	<0.001	-12	-70	-22	Cerebellum_6_L
				<0.001	0.027	9.88	6.12	<0.001	12	-70	-20	Cerebellum_6_R
<0.001	<0.001	82	<0.001	<0.001	0.070	9.14	5.88	<0.001	56	10	26	Frontal_Inf_Oper_R
				0.006	0.234	7.86	5.42	<0.001	56	10	38	Precentral_R
<0.001	<0.001	141	<0.001	0.001	0.092	8.89	5.80	<0.001	-34	-52	-24	Cerebellum_6_L
				0.002	0.117	8.47	5.65	<0.001	-28	-62	-24	Cerebellum_6_L
<0.001	<0.001	76	<0.001	0.001	0.092	8.87	5.79	<0.001	-28	-52	56	Parietal_Sup_L
				0.011	0.341	7.57	5.31	<0.001	-30	-44	48	Parietal_Inf_L
<0.001	<0.001	200	<0.001	0.001	0.092	8.77	5.76	<0.001	32	-48	-28	Cerebellum_6_R
				0.013	0.382	7.49	5.28	<0.001	34	-40	-34	Cerebellum_6_R
<0.001	<0.001	36	<0.001	0.001	0.092	8.73	5.74	<0.001	16	-54	-18	Cerebellum_4_5_R
<0.001	<0.001	28	<0.001	0.001	0.101	8.63	5.71	<0.001	26	-58	-54	Cerebellum_8_R
<0.001	<0.001	62	<0.001	0.001	0.113	8.51	5.67	<0.001	38	-62	-16	Fusiform_R
				0.002	0.117	8.45	5.64	<0.001	42	-72	-12	Occipital_Inf_R
<0.001	<0.001	21	<0.001	0.002	0.117	8.41	5.63	<0.001	-46	-68	4	Occipital_Mid_L
<0.001	<0.001	141	<0.001	0.002	0.130	8.33	5.60	<0.001	22	-56	50	Location not in atlas
				0.002	0.130	8.30	5.59	<0.001	30	-48	48	Parietal_Sup_R
				0.007	0.266	7.76	5.39	<0.001	36	-40	42	SupraMarginal_R
<0.001	<0.001	29	<0.001	0.004	0.170	8.09	5.51	<0.001	44	-50	-34	Cerebellum_Crus_1_R

<0.001	<0.001	59	<0.001	0.004	0.178	8.04	5.49	<0.001	-22	-66	-52	Cerebellum_8_L
<0.001	0.006	12	0.003	0.004	0.190	7.99	5.47	<0.001	10	-16	8	Thal_MDl_R
0.001	0.043	6	0.028	0.009	0.319	7.63	5.33	<0.001	-22	-2	6	Putamen_L
<0.001	<0.001	34	<0.001	0.009	0.319	7.63	5.33	<0.001	18	-64	-54	Cerebellum_8_R
0.001	0.300	7	0.019	0.023	0.545	7.23	5.17	<0.001	20	2	62	Frontal_Sup_2_R
0.001	0.030	7	0.019	0.024	0.560	7.21	5.16	<0.001	52	12	8	Frontal_Inf_Oper_R
0.001	0.030	7	0.019	0.025	0.568	7.19	5.16	<0.001	-44	-36	40	Parietal_Inf_L

Table S2: Significant clusters and the respective local maxima in the tTIS$_{Sham}$, Reinf$_{ON}$ condition. Related to Figure S6. Regions were identified with the Automated Anatomical Labelling atlas 3 (AAL3[139]). Significant clusters were selected for corrected voxel-wise family wise error (FWE), p=0.05, and corrected cluster-based false discovery rate (FDR), p=0.05.

10. Correlation between effect of tTIS$_{80Hz}$ on reinforcement motor learning and modulation of whole-brain activity

Cluster-level				Peak-level					x	y	z	Region
p$_{FWE\text{-}corr}$	q$_{FDR\text{-}corr}$	k$_E$	P$_{uncorr}$	p$_{FWE\text{-}corr}$	q$_{FDR\text{-}corr}$	T	(Z$_E$)	P$_{uncorr}$				
0.003	**0.005**	**157**	**<0.001**	**0.027**	**0.065**	**7.29**	**5.14**	**<0.001**	**10**	**18**	**0**	Caudate_R
				0.639	0.678	5.38	4.25	<0.001	0	0	10	Location not in atlas
				0.921	0.757	4.89	3.98	<0.001	6	6	2	Location not in atlas
0.007	**0.005**	**138**	**<0.001**	**0.693**	**0.678**	**5.30**	**4.21**	**<0.001**	**-16**	**14**	**6**	Location not in atlas
				0.923	0.757	4.88	3.98	<0.001	-22	14	-2	Putamen_L
				1.000	0.810	4.26	3.60	<0.001	-18	8	-6	Putamen_L

Table S3. Significant clusters for the correlation between the behavioural and neural effects of tTIS$_{80Hz}$ (vs. tTIS$_{20Hz}$). Related to Figure 3B. Two significant clusters were found with several local maxima. Notably, the left cluster also encompassed a portion of the left caudate (related to Figure 3). Regions were identified with the Automated Anatomical Labelling atlas 3 (AAL3[139]). Significant clusters were selected for uncorrected voxel-wise family wise error (FWE), p=0.001, and corrected cluster-based false discovery rate (FDR), p=0.05.

11. Control analysis on striatum to frontal cortex effective connectivity

The connectivity analysis showed that tTIS$_{80Hz}$, but not tTIS$_{20Hz}$, increased striatum to

frontal effective connectivity and that this effect depended on the type of network considered

60

1244   (reward vs. motor) and on the presence of reinforcement (Figure 4). In this analysis we considered

1245   effective connectivity between the motor striatum and M1 and SMA for the motor network and the

1246   limbic striatum with ACC and vmPFC for the reward network, based on a large body of

1247   literature[11,12,135,136] (see Methods for a detailed justification of the ROIs). To verify whether our

1248   results depended on the specific frontal ROIs included in the analysis, we performed a new

1249   analysis. More specifically, we decomposed connectivity in each network for each frontal cortical

1250   area (M1 and SMA in the motor network and ACC and vmPFC in the reward network) and ran two

1251   separate LMMs on each network with $tTIS_{TYPE}$, $Reinf_{TYPE}$ as well as ROI_{TYPE} (M1 or SMA for the

1252   LMM run on the motor network and ACC or vmPFC for the reward network) as fixed effects.

1253   Consistent with our initial findings, we found effects of $tTIS_{TYPE}$ on both LMMs (motor network:

1254 $F_{(2,1089.7)}=3.12$; p=0.044 and reward network: $F_{(2,1112)}=6.78$; p=0.0012). Moreover, there was a

1255   significant $tTIS_{TYPE}$ x $Reinf_{TYPE}$ interaction in the motor network ($F_{(2,1112)}=3.36$; p=0.035), which was

1256   at the trend level in the reward network ($F_{(2,1113.8)}=2.37$; p=0.094). Most importantly, these effects

1257   were not modulated by ROI_{TYPE} in any network ($tTIS_{TYPE}$ x $Reinf_{TYPE}$ x ROI_{TYPE} in motor network:

1258 $F_{(2,1112)}=0.83$; p=0.44, in reward network: $F_{(2,1112)}=0.61$; p=0.54). This analysis suggests that the

1259   main connectivity findings were not influenced by the specific frontal ROIs considered in the

1260   analysis.

1261

1262

1263   **12. Relationship between the neural and behavioural effects of tTIS$_{80Hz}$ and impulsivity**

1264

1265   Characterising individual factors that influence responsiveness to brain stimulation is an

1266   important line of research both for fundamental neuroscience but also to determine profiles of

1267   responders for future clinical translation. Based on previous literature linking striatal gamma

1268   oscillatory mechanisms and impulsivity[72], we explored the possibility that impulsivity influences

1269   responsiveness to striatal tTIS$_{80Hz}$ (**Figure S7**).

1270   First, we exploited the BOLD data and asked if inter-individual variability in the neural

1271   effects of $tTIS_{80Hz}$ during reinforcement motor learning (i.e., in the $Reinf_{ON}$ condition) was related

1272   to impulsivity at the whole-brain level. Impulsivity was evaluated by a well-established independent

1273   delay-discounting questionnaire performed at the beginning of the experiment[75,76]. Strikingly, this

1274   analysis revealed that impulsivity was associated to the effect of $tTIS_{80Hz}$ (with respect to $tTIS_{20Hz}$)

1275   specifically in the left caudate nucleus (Figure S7A, Table S4). No other clusters were found. As

1276   such, the most impulsive participants exhibited an increase of left caudate activity with $tTIS_{80Hz}$

1277   (compared to $tTIS_{20Hz}$) while the least impulsive ones rather presented a decrease of BOLD signal,

1278   consistent with the idea that impulsivity modulates the neuronal responsiveness to tTIS (R^2=0.47;

1279   p<0.001; Figure S7B). No significant clusters of correlation were found for the $tTIS_{80Hz} - tTIS_{Sham}$

1280   contrast, neither for the control $tTIS_{20Hz} - tTIS_{Sham}$ contrast. Hence, this analysis suggests that the

1281   effect of $tTIS_{80Hz}$ on caudate activity depends on participants' impulsivity.

1282   As a second step, we aimed at evaluating the association between impulsivity and the

1283   increased striatum to motor cortex connectivity observed with $tTIS_{80Hz}$, in the presence of

1284   reinforcement. Notably, such pattern of increased connectivity in fronto-striatal circuits has been

1285   described as a pathophysiological mechanism in multiple neuro-psychiatric disorders involving

1286   impulsivity[101-104]. Hence, we first asked if striatum to motor cortex connectivity was related to

1287   impulsivity during reinforcement motor learning in the absence of stimulation (i.e., in the $tTIS_{Sham}$

1288   condition). Indeed, we found a significant positive relationship between impulsivity and striatum to

1289   motor cortex connectivity (robust linear regression: R^2=0.10; p=0.0038), in line with previous

1290   results[101-104]. Then, we evaluated whether the increase of connectivity observed with $tTIS_{80Hz}$ in

1291   the $Reinf_{ON}$ condition (Figure 4A) could be related to impulsivity. Indeed, we found that the effect

1292   of $tTIS_{80Hz}$ on connectivity was negatively correlated to impulsivity both when contrasting $tTIS_{80Hz}$

1293   with $tTIS_{Sham}$ (R^2=0.19; p=0.043, Figure S7C, left) and with $tTIS_{20Hz}$ (R^2=0.28; p=0.021, Figure S7C,

1294   middle): participants with the largest increase in connectivity with $tTIS_{80Hz}$ in the $Reinf_{ON}$ condition

1295 were also the least impulsive ones. Such correlation was absent when contrasting tTIS$_{20Hz}$ and

1296 tTIS$_{Sham}$ (R^2=0.0031; p=0.31, Figure S7C, right), but also when considering the same contrasts in

1297 the reward instead of the motor network (p=0.93 and p=0.86 for the tTIS$_{80Hz}$-tTIS$_{Sham}$ and tTIS$_{80Hz}$-

1298 tTIS$_{20Hz}$ contrasts, respectively). Hence, striatum to motor cortex effective connectivity during the

1299 task was positively correlated to impulsivity, but the change in connectivity induced by tTIS$_{80Hz}$

1300 was rather negatively associated with impulsivity. This may be due to a ceiling effect in the most

1301 impulsive participants: exhibiting initially high levels of connectivity may leave less room for further

1302 modulation by tTIS$_{80Hz}$. These results suggest that inter-individual variability in impulsivity might

1303 influence neural responses to striatal tTIS$_{80Hz}$.
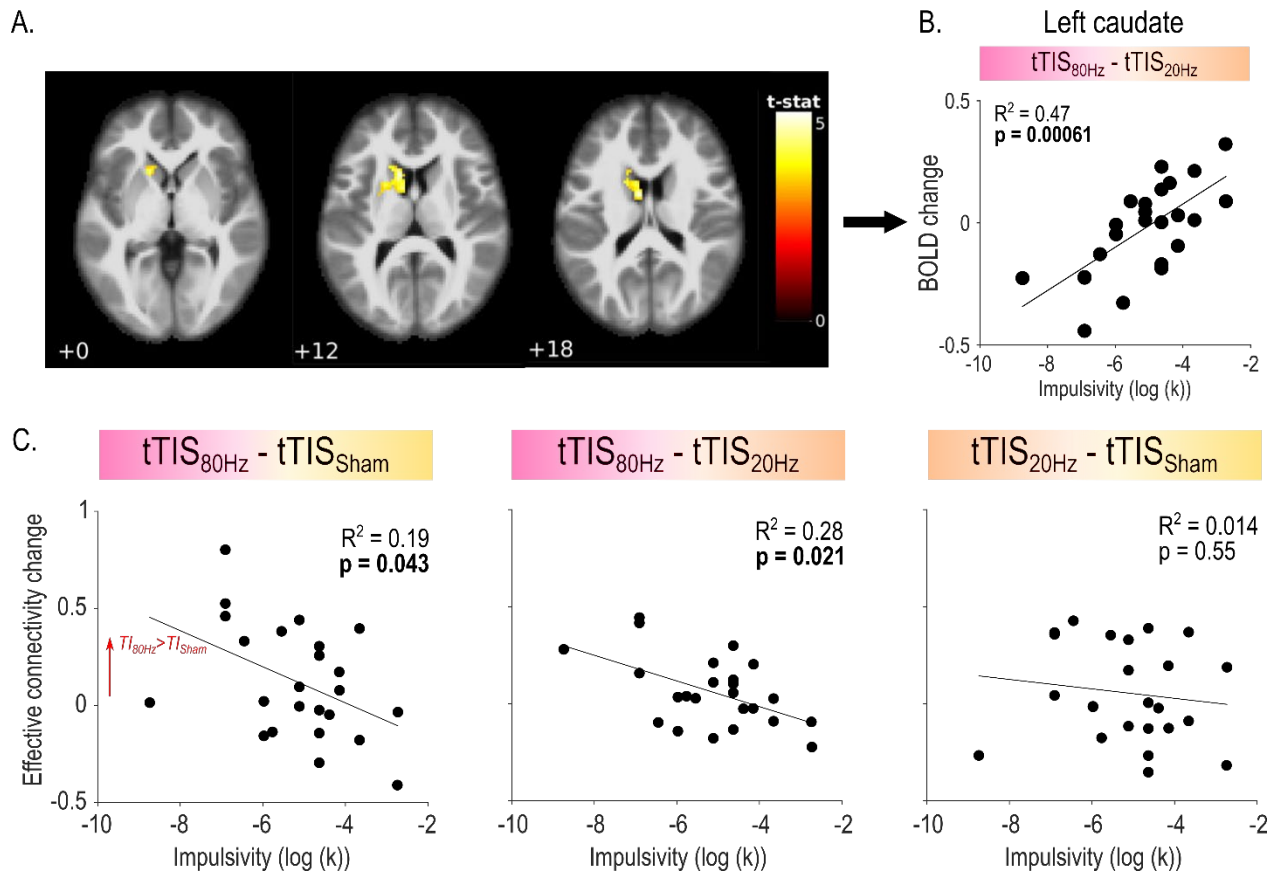
1304

1305 **Figure S7. Relationship between impulsivity and the neural effects of tTIS$_{80Hz}$. A)**
1306 **Whole-brain correlation between the neural effects of tTIS$_{80Hz}$ (with respect to tTIS$_{20Hz}$) and**
1307 **impulsivity.** Correlation between tTIS-related modulation of striatal activity (tTIS$_{80Hz}$ − tTIS$_{20Hz}$)
1308 during reinforcement motor learning (Reinf$_{ON}$) and individual impulsivity levels. A single significant
1309 cluster of correlation was found in left caudate (uncorrected voxel-wise FWE: p=0.001, and

1310 corrected cluster-based FDR: p=0.05). **B) Correlation between left caudate activity and**
1311 **impulsivity.** A positive correlation was found showing that participants with higher levels of
1312 impulsivity exhibited stronger activation of the left caudate in the $tTIS_{80Hz}$ (with respect to $tTIS_{20Hz}$).
1313 **C) Correlations between impulsivity and tTIS-related modulation of effective connectivity.**
1314 Impulsivity was associated to the neural effects of $tTIS_{80Hz}$ both when contrasting to $tTIS_{Sham}$ (left)
1315 and $tTIS_{20Hz}$ (middle), but was not correlated to the effect of $tTIS_{20Hz}$ (right).

1316

Cluster-level				Peak-level					x	y	z	Region
$p_{FWE\text{-}corr}$	$q_{FDR\text{-}corr}$	k_E	P_{uncorr}	$p_{FWE\text{-}corr}$	$q_{FDR\text{-}corr}$	T	(Z_E)	P_{uncorr}				
<0.001	<0.001	254	<0.001	0.707	0.524	5.29	4.20	<0.001	-8	0	18	Location not in atlas
				0.719	0.524	5.27	4.19	<0.001	-14	16	16	Caudate_L
				0.971	0.620	4.72	3.88	<0.001	-16	16	0	Location not in atlas

1317 **Table S4. Significant clusters for the correlation between impulsivity and effects of**
1318 **$tTIS_{80Hz}$ on BOLD activity (vs. $tTIS_{20Hz}$).** Related to Figure S7A. One significant cluster
1319 encompassing the left caudate nucleus was found. Regions were identified with AAL3[139].

1320

1321 As a last step, we verified if impulsivity was also predictive of the behavioural effects of

1322 $tTIS_{80Hz}$ on reinforcement motor learning. We did not find any significant correlation between

1323 impulsivity and the effect of $tTIS_{80Hz}$ on motor learning ($tTIS_{80Hz}$ – $tTIS_{Sham}$: R^2=0.098; p=0.17;

1324 $tTIS_{80Hz}$ – $tTIS_{20Hz}$: R^2=0.11; p=0.21). Hence, impulsivity was associated to the neural, but not the

1325 behavioural effects of $tTIS_{80Hz}$.

1326

1327 Overall, we found that impulsivity was associated to $tTIS_{80Hz}$-related BOLD changes

1328 specifically in the left caudate and to changes of effective connectivity between the motor striatum

1329 and motor cortex during reinforcement motor learning. Hence, a possibility is that the differences

1330 in endogenous striatal gamma-related activity that have been associated to impulsive behaviour

1331 in animal models[72–74], influence the neural effects of $tTIS_{80Hz}$. If this is the case, impulsivity could

1332 constitute a behavioural factor allowing to determine responsiveness to striatal $tTIS_{80Hz}$.

1333   Conversely, an interesting avenue for future research could aim at determining whether impulsivity

1334   can be modulated by striatal $tTIS_{80Hz}$.

1335

1336

1337   **13. Imaging quality control**

1338

1339   A threshold of 0.5 was chosen to discard subjects showing more than 40% of voxels with

1340   framewise displacement FD higher than this threshold. In the current study cohort, no subject

1341   exceeded the limit value, thus the whole dataset could be used. Furthermore, successful cleaning

1342   of the data was ensured by visual checking the preprocessing results. In particular, good

1343   registration between anatomical and functional images and normalization to standard space were

1344   checked. Signal to noise ratio analysis showed significantly higher tSNR values underneath the

1345   stimulating electrodes ($F_{(1,1122)}=249.25$, $p<0.001$; **Figure S5**). Moreover, an additional analysis

1346   showed that this effect was not influenced by the $tTIS_{TYPE}$ ($Sphere_{LOCATION}$ x $tTIS_{TYPE}$:

1347 $F_{(2,1118)}=0.0169$, $p=0.98$). This result suggests that the stimulation did not introduce additional

1348   noise to the MR images. In summary, all controls confirmed the good quality of the imaging data.
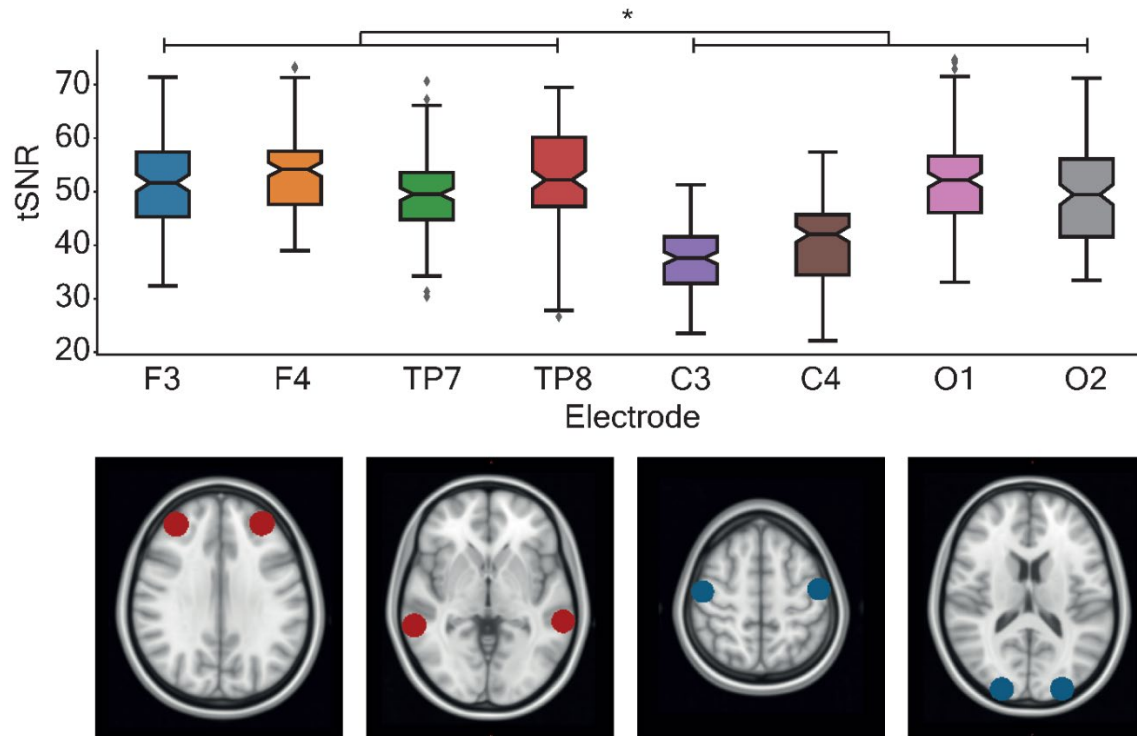
Figure S8. Total signal to noise ratio (tSNR). Total signal to noise ratio investigation. On the top panel, the average tSNR is shown within spheres of 10mm radius underneath the 4 stimulation electrodes (F3, F4, TP7 and TP8) and underneath other 4 locations more distal from the electrodes (C3, C4, O1 and O2). A significant higher tSNR was found underneath the electrodes with respect to the distal locations ($F_{(1,1122)}$=249.25, p<0.001). This indicates that there was no reduction of the tSNR due to the presence of electrical current. On the bottom panel, the location of the spheres from where the average tSNRs were extracted: F3 and F4 in red in the first image from the left, TP7 and TP8 in red on the second image from the left, C3 and C4 in blue on the third image from the left, O1 and O2 in blue on the forth image from the left.

Acknowledgements

Competing interests

E.N. is co-founder of TI Solutions AG, a company committed to producing hardware and software solutions to support tTIS research.

Data and code availability statement

The datasets generated during the current study and the code used to analyse them are available from the corresponding author on reasonable request.

References

1. Neftci, E. O. & Averbeck, B. B. Reinforcement learning in artificial and biological systems. *Nat. Mach. Intell.* **1**, 133–143 (2019).

2. Schultz, W. Neuronal Reward and Decision Signals: From Theories to Data. *Physiol. Rev.* **95**, 853–951 (2015).

3. Dhawale, A. K., Smith, M. A. & Ölveczky, B. P. The Role of Variability in Motor Learning. *Annu. Rev. Neurosci.* **40**, 479–498 (2017).

4. Vassiliadis, P. *et al.* Reward boosts reinforcement-based motor learning. *iScience* **24**, 102821 (2021).

5. Spampinato, D. & Celnik, P. Multiple Motor Learning Processes in Humans: Defining Their Neurophysiological Bases. *Neuroscientist* **27**, 246–267 (2021).

6. Huang, V. S., Haith, A., Mazzoni, P. & Krakauer, J. W. Rethinking Motor Learning and Savings in Adaptation Paradigms: Model-Free Memory for Successful Actions Combines with Internal Models. *Neuron* **70**, 787–801 (2011).

7. Galea, J. M., Mallia, E., Rothwell, J. & Diedrichsen, J. The dissociable effects of punishment and reward on motor learning. *Nat. Neurosci.* **18**, 597–602 (2015).

8. Therrien, A. S., Wolpert, D. M. & Bastian, A. J. Effective Reinforcement learning following cerebellar damage requires a balance between exploration and motor noise. *Brain* **139**, 101–114 (2016).

9. Vassiliadis, P., Derosiere, G. & Duque, J. Beyond Motor Noise : Considering Other Causes of Impaired Reinforcement Learning in Cerebellar Patients. *Eneuro* **6**, 1–4 (2019).

1402   10.   Widmer, M. *et al.* Reward During Arm Training Improves Impairment and Activity

1403   After Stroke: A Randomized Controlled Trial. *Neurorehabil. Neural Repair* **0**,

1404   154596832110628 (2021).

1405   11.   Bartra, O., McGuire, J. T. & Kable, J. W. The valuation system: A coordinate-

1406   based meta-analysis of BOLD fMRI experiments examining neural correlates of

1407   subjective value. *Neuroimage* **76**, 412–427 (2013).

1408   12.   Hardwick, R. M., Rottschy, C., Miall, R. C. & Eickhoff, S. B. A quantitative meta-

1409   analysis and review of motor learning in the human brain. *Neuroimage* **67**, 283–

1410   297 (2013).

1411   13.   Haber, S. N. Corticostriatal circuitry. *Dialogues Clin. Neurosci.* **18**, 7–21 (2016).

1412   14.   Balleine, B. W., Delgado, M. R. & Hikosaka, O. The role of the dorsal striatum in

1413   reward and decision-making. *J. Neurosci.* **27**, 8161–8165 (2007).

1414   15.   Piray, P., den Ouden, H. E. M., van der Schaaf, M. E., Toni, I. & Cools, R.

1415   Dopaminergic modulation of the functional ventrodorsal architecture of the human

1416   striatum. *Cereb. Cortex* **27**, 485–495 (2017).

1417   16.   Hori, Y. *et al.* Ventral striatum links motivational and motor networks during

1418   operant-conditioned movement in rats. *Neuroimage* **184**, 943–953 (2019).

1419   17.   Wachter, T., Lungu, O. V., Liu, T., Willingham, D. T. & Ashe, J. Differential Effect

1420   of Reward and Punishment on Procedural Learning. *J. Neurosci.* **29**, 436–443

1421   (2009).

1422   18.   Widmer, M., Ziegler, N., Held, J., Luft, A. & Lutz, K. Rewarding feedback promotes

1423   motor skill consolidation via striatal activity. in *Progress in Brain Research* **5**, 303–

1424   323 (2016).

1425   19.   Berke, J. D. Fast oscillations in cortical-striatal networks switch frequency

1426   following rewarding events and stimulant drugs. *Eur. J. Neurosci.* **30**, 848–859

1427   (2009).

1428   20.   van der Meer, M. A. A. *et al.* Integrating early results on ventral striatal gamma

1429   oscillations in the rat. *Front. Neurosci.* **4**, 1–12 (2010).

1430   21.   van der Meer, M. A. A. & Redish, A. D. Low and high gamma oscillations in rat

1431   ventral striatum have distinct relationships to behavior, reward, and spiking activity

1432   on a learned spatial decision task. *Front. Integr. Neurosci.* **3**, 1–19 (2009).

1433   22.   Dwiel, L. L., Khokhar, J. Y., Connerney, M. A., Green, A. I. & Doucette, W. T.

1434   Finding the balance between model complexity and performance: Using ventral

1435   striatal oscillations to classify feeding behavior in rats. *PLoS Comput. Biol.* **15**, 1–

1436   19 (2019).

1437   23.   Matsumoto, J. *et al.* Neuronal responses in the nucleus accumbens shell during

1438   sexual behavior in male rats. *J. Neurosci.* **32**, 1672–1686 (2012).

1439   24.   Kalenscher, T., Lansink, C. S., Lankelma, J. V. & Pennartz, C. M. A. Reward-

1440   associated gamma oscillations in ventral striatum are regionally differentiated and

1441   modulate local firing activity. *J. Neurophysiol.* **103**, 1658–1672 (2010).

1442   25.   Cohen, M. X. *et al.* Good vibrations: Cross-frequency coupling in the human

1443   nucleus accumbens during reward processing. *J. Cogn. Neurosci.* **21**, 875–889

1444   (2009).

1445   26.   Sepe-Forrest, L., Carver, F. W., Quentin, R., Holroyd, T. & Nugent, A. C. Basal

1446   ganglia activation localized in MEG using a reward task. *Neuroimage: Reports* **1**,

1447   100034 (2021).

1448   27.   Herrojo-Ruiz, M. *et al.* Involvement of human internal globus pallidus in the early

1449   modulation of cortical error-related activity. *Cereb. Cortex* **24**, 1502–1517 (2014).

1450   28.   Jenkinson, N. & Brown, P. New insights into the relationship between dopamine,

1451   beta oscillations and motor function. *Trends Neurosci.* **34**, 611–618 (2011).

1452   29.   Brown, P. Abnormal oscillatory synchronisation in the motor system leads to

1453   impaired movement. *Curr. Opin. Neurobiol.* **17**, 656–664 (2007).

1454   30.   McCarthy, M. M. *et al.* Striatal origin of the pathologic beta oscillations in

1455   Parkinson's disease. *Proc. Natl. Acad. Sci. U. S. A.* **108**, 11620–11625 (2011).

1456   31.   Kondabolu, K. *et al.* Striatal cholinergic interneurons generate beta and gamma

1457   oscillations in the corticostriatal circuit and produce motor deficits. *Proc. Natl.*

1458   *Acad. Sci. U. S. A.* **113**, 3159–3168 (2016).

1459   32.   Silberstein, P. *et al.* Cortico-cortical coupling in Parkinson's disease and its

1460   modulation by therapy. *Brain* **128**, 1277–1291 (2005).

1461   33.   Williams, Z. M. & Eskandar, E. N. Selective enhancement of associative learning

1462   by microstimulation of the anterior caudate. *Nat. Neurosci.* **9**, 562–568 (2006).

1463   34.   Nakamura, K. & Hikosaka, O. Facilitation of saccadic eye movements by

1464   postsaccadic electrical stimulation in the primate caudate. *J. Neurosci.* **26**, 12885–

1465   12895 (2006).

1466   35.   Deng, Z. De, Lisanby, S. H. & Peterchev, A. V. Electric field depth-focality tradeoff

1467   in transcranial magnetic stimulation: Simulation comparison of 50 coil designs.

71

1468   *Brain Stimul.* **6**, 1–13 (2013).

1469   36.   Wagner, T. *et al.* Transcranial direct current stimulation: A computer-based human

1470   model study. *Neuroimage* **35**, 1113–1124 (2007).

1471   37.   Nickchen, K. *et al.* Reversal learning reveals cognitive deficits and altered

1472   prediction error encoding in the ventral striatum in Huntington's disease. *Brain*

1473   *Imaging Behav.* **11**, 1862–1872 (2017).

1474   38.   Schmidt, L. *et al.* Disconnecting force from money: Effects of basal ganglia

1475   damage on incentive motivation. *Brain* **131**, 1303–1310 (2008).

1476   39.   Seymour, B. *et al.* Deep brain stimulation of the subthalamic nucleus modulates

1477   sensitivity to decision outcome value in Parkinson's disease. *Sci. Rep.* **6**, 1–12

1478   (2016).

1479   40.   Atkinson-Clement, C. *et al.* Effects of subthalamic nucleus stimulation and

1480   levodopa on decision-making in Parkinson's disease. *Mov. Disord.* **34**, 377–385

1481   (2019).

1482   41.   Grossman, N. *et al.* Noninvasive Deep Brain Stimulation via Temporally Interfering

1483   Electric Fields. *Cell* **169**, 1029-1041.e16 (2017).

1484   42.   Song, S., Zhang, J., Tian, Y., Wang, L. & Wei, P. Temporal Interference

1485   Stimulation Regulates Eye Movements and Neural Activity in the Mice Superior

1486   Colliculus. *Proc. Annu. Int. Conf. IEEE Eng. Med. Biol. Soc. EMBS* 6231–6234

1487   (2021). doi:10.1109/EMBC46164.2021.9629968

1488   43.   Esmaeilpour, Z., Kronberg, G., Reato, D., Parra, L. C. & Bikson, M. Temporal

1489   interference stimulation targets deep brain regions by modulating neural

1490   oscillations. *Brain Stimul.* **14**, 55–65 (2021).

1491   44.   Rampersad, S. *et al.* Prospects for transcranial temporal interference stimulation

1492   in humans: A computational study. *Neuroimage* **202**, 116124 (2019).

1493   45.   von Conta, J. *et al.* Interindividual variability of electric fields during transcranial

1494   temporal interference stimulation (tTIS). *Sci. Rep.* **11**, 1–12 (2021).

1495   46.   Cao, J., Doiron, B., Goswami, C. & Grover, P. The mechanics of temporal

1496   interference stimulation. *bioRxiv* 1–6 (2020). doi:10.1101/2020.04.23.051870

1497   47.   Mirzakhalili, E., Barra, B., Capogrosso, M. & Lempka, S. F. Biophysics of

1498   Temporal Interference Stimulation. *Cell Syst.* **11**, 557-572.e5 (2020).

1499   48.   von Conta, J. *et al.* Benchmarking the effects of transcranial temporal interference

1500   stimulation (tTIS) in humans. *Cortex* **154**, 299–310 (2022).

1501   49.   Ma, R. *et al.* High Gamma and Beta Temporal Interference Stimulation in the

1502   Human Motor Cortex Improves Motor Functions. *Front. Neurosci.* **15**, 1–11 (2022).

1503   50.   Hutcheon, B. & Yarom, Y. Resonance, oscillation and the intrinsic frequency

1504   preferences of neurons. *Trends Neurosci.* **23**, 216–222 (2000).

1505   51.   Acerbo, E. *et al.* Focal non-invasive deep-brain stimulation with temporal

1506   interference for the suppression of epileptic biomarkers. *Front. Neurosci.* **16**, 1–12

1507   (2022).

1508   52.   Wessel, M. J. *et al.* LTP-like noninvasive striatal brain stimulation enhances

1509   striatal activity and motor skill learning in humans. *bioRxiv* 1–30 (2022).

1510   doi:10.1101/2022.10.28.514204

1511   53.   Violante, I. R. *et al.* Non-invasive temporal interference electrical stimulation of the

1512   human hippocampus. *biorXiv* (2022). doi:10.1101/2022.09.14.507625

1513   54.   Abe, M. *et al.* Reward improves long-term retention of a motor memory through

1514   induction of offline memory gains. *Curr. Biol.* **21**, 557–562 (2011).

1515   55.   Steel, A., Silson, E. H., Stagg, C. J. & Baker, C. I. The impact of reward and

1516   punishment on skill learning depends on task demands. *Sci. Rep.* **6**, 1–9 (2016).

1517   56.   Vassiliadis, P., Lete, A., Duque, J. & Derosiere, G. Reward timing matters in motor

1518   learning. *iScience* **25**, 104290 (2022).

1519   57.   Izawa, J. & Shadmehr, R. Learning from sensory and reward prediction errors

1520   during motor adaptation. *PLoS Comput. Biol.* **7**, 1–12 (2011).

1521   58.   Mawase, F., Uehara, S., Bastian, A. J. & Celnik, P. Motor Learning Enhances

1522   Use-Dependent Plasticity. *J. Neurosci.* **37**, 2673–2685 (2017).

1523   59.   Iacono, M. I. *et al.* MIDA: A multimodal imaging-based detailed anatomical model

1524   of the human head and neck. *PLoS One* **10**, (2015).

1525   60.   Jiang, T. Brainnetome: A new -ome to understand the brain and its disorders.

1526   *Neuroimage* **80**, 263–272 (2013).

1527   61.   Areshenkoff, C. N., de Brouwer, A. J., Gale, D. J., Nashed, J. Y. & Gallivan, J. P.

1528   Separate and shared low-dimensional neural architectures for error-based and

1529   reinforcement motor learning. *biorXiv* (2022). doi:10.1101/2022.08.16.504134

1530   62.   Cashaback, J. G. A., McGregor, H. R., Mohatarem, A. & Gribble, P. L.

1531   Dissociating error-based and reinforcement-based loss functions during

1532   sensorimotor learning. *PLoS Comput. Biol.* **13**, 1–28 (2017).

1533   63.   Floyer-Lea, A. & Matthews, P. M. Changing brain networks for visuomotor control

1534   with increased movement automaticity. *J. Neurophysiol.* **92**, 2405–2412 (2004).

1535   64.   Floyer-Lea, A. & Matthews, P. M. Distinguishable brain activation networks for

1536   short- and long-term motor skill learning. *J. Neurophysiol.* **94**, 512–518 (2005).

1537   65.   Graybiel, A. M. & Grafton, S. T. The striatum: Where skills and habits meet. *Cold*

1538   *Spring Harb. Perspect. Biol.* **7**, 1–14 (2015).

1539   66.   McLaren, D. G., Ries, M. L., Xu, G. & Johnson, S. C. A generalized form of

1540   context-dependent psychophysiological interactions (gPPI): A comparison to

1541   standard approaches. *Neuroimage* **61**, 1277–1286 (2012).

1542   67.   Codol, O., Holland, P. J., Manohar, S. G. & Galea, J. M. Reward-Based

1543   Improvements in Motor Control Are Driven by Multiple Error-Reducing

1544   Mechanisms. *J. Neurosci.* **40**, 3604–3620 (2020).

1545   68.   Sidarta, A., Vahdat, S., Bernardi, N. F. & Ostry, D. J. Somatic and reinforcement-

1546   based plasticity in the initial stages of human motor learning. *J. Neurosci.* **36**,

1547   11682–11692 (2016).

1548   69.   Krause, M. R., Vieira, P. G., Csorba, B. A., Pilly, P. K. & Pack, C. C. Transcranial

1549   alternating current stimulation entrains single-neuron activity in the primate brain.

1550   *Proc. Natl. Acad. Sci. U. S. A.* **116**, 5747–5755 (2019).

1551   70.   Shirer, W. R., Ryali, S., Rykhlevskaia, E., Menon, V. & Greicius, M. D. Decoding

1552   subject-driven cognitive states with whole-brain connectivity patterns. *Cereb.*

1553   *Cortex* **22**, 158–165 (2012).

1554   71.   Morishita, T. & Hummel, F. C. Non-invasive Brain Stimulation (NIBS) in Motor

1555   Recovery After Stroke: Concepts to Increase Efficacy. *Curr. Behav. Neurosci.*

1556   *Reports* **4**, 280–289 (2017).

1557   72.   Donnelly, N. A. *et al.* Oscillatory activity in the medial prefrontal cortex and nucleus

1558   accumbens correlates with impulsivity and reward outcome. *PLoS One* **9**, 14–17

1559   (2014).

1560   73.   Schall, T. A., Wright, W. J. & Dong, Y. Nucleus accumbens fast-spiking

1561   interneurons in motivational and addictive behaviors. *Mol. Psychiatry* **26**, 234–246

1562   (2021).

1563   74.   Pisansky, M. T. *et al.* Nucleus Accumbens Fast-Spiking Interneurons Constrain

1564   Impulsive Action. *Biol. Psychiatry* **86**, 836–847 (2019).

1565   75.   Kirby, K. N., Petry, N. M. & Bickel, W. K. Heroin addicts have higher discount rates

1566   for delayed rewards than non-drug-using controls. *J. Exp. Psychol. Gen.* **128**, 78–

1567   87 (1999).

1568   76.   Mitchell, J. M., Fields, H. L., D'Esposito, M. & Boettiger, C. A. Impulsive

1569   responding in alcoholics. *Alcohol. Clin. Exp. Res.* **29**, 2158–2169 (2005).

1570   77.   Catanese, J., Carmichael, J. E. & van der Meer, M. A. A. Low- and high-gamma

1571   oscillations deviate in opposite directions from zero-phase synchrony in the limbic

1572   corticostriatal loop. *J. Neurophysiol.* **116**, 5–17 (2016).

1573   78.   Rothé, M., Quilodran, R., Sallet, J. & Procyk, E. Coordination of high gamma

1574   activity in anterior cingulate and lateral prefrontal cortical areas during adaptation.

1575   *J. Neurosci.* **31**, 11110–11117 (2011).

1576   79.   Del Arco, A., Park, J., Wood, J., Kim, Y. & Moghaddam, B. Adaptive encoding of

1577   outcome prediction by prefrontal cortex ensembles supports behavioral flexibility.

1578   *J. Neurosci.* **37**, 8363–8373 (2017).

1579   80.   Yoshimoto, A., Shibata, Y., Kudara, M., Ikegaya, Y. & Matsumoto, N.

1580   Enhancement of Motor Cortical Gamma Oscillations and Sniffing Activity by

1581   Medial Forebrain Bundle Stimulation Precedes Locomotion. *eNeuro* **9**, 1–14

1582   (2022).

1583   81.   Grover, S., Nguyen, J. A., Viswanathan, V. & Reinhart, R. M. G. High-frequency

1584   neuromodulation improves obsessive–compulsive behavior. *Nat. Med.* **27**, 232–

1585   238 (2021).

1586   82.   Krause, M. R., Vieira, P. G., Thivierge, J. P. & Pack, C. C. Brain stimulation

1587   competes with ongoing oscillations for control of spike timing in the primate brain.

1588   *PLoS Biol.* **20**, 1–27 (2022).

1589   83.   Courtemanche, R., Fujii, N. & Graybiel, A. M. Synchronous, Focally Modulated β-

1590   Band Oscillations Characterize Local Field Potential Activity in the Striatum of

1591   Awake Behaving Monkeys. *J. Neurosci.* **23**, 11741–11752 (2003).

1592   84.   Costa, R. M. *et al.* Rapid Alterations in Corticostriatal Ensemble Coordination

1593   during Acute Dopamine-Dependent Motor Dysfunction. *Neuron* **52**, 359–369

1594   (2006).

1595   85.   Engel, A. K. & Fries, P. Beta-band oscillations-signalling the status quo? *Curr.*

1596   *Opin. Neurobiol.* **20**, 156–165 (2010).

1597   86.   Uehara, S., Mawase, F. & Celnik, P. Learning similar actions by reinforcement or

1598   sensory-prediction errors rely on distinct physiological mechanisms. *Cereb. Cortex*

1599   **28**, 3478–3490 (2018).

87. Mathis, M. W., Mathis, A. & Uchida, N. Somatosensory Cortex Plays an Essential Role in Forelimb Motor Adaptation in Mice. *Neuron* **93**, 1493-1503.e6 (2017).

88. Brücke, C. *et al.* Scaling of movement is related to pallidal γ oscillations in patients with dystonia. *J. Neurosci.* **32**, 1008–1019 (2012).

89. Soderstrom, N. C. & Bjork, R. A. Learning Versus Performance: An Integrative Review. *Perspect. Psychol. Sci.* **10**, 176–199 (2015).

90. Spampinato, D. A., Satar, Z. & Rothwell, J. C. Combining reward and M1 transcranial direct current stimulation enhances the retention of newly learnt sensorimotor mappings. *Brain Stimul.* 1–8 (2019). doi:10.1016/j.brs.2019.05.015

91. Shmuelof, L. *et al.* Overcoming Motor 'Forgetting' Through Reinforcement Of Learned Actions. *J. Neurosci.* **32**, 14617-14621a (2012).

92. Dhawale, A. K., Miyamoto, Y. R., Smith, M. A. & Ölveczky, B. P. Adaptive Regulation of Motor Variability. *Curr. Biol.* **29**, 3551-3562.e7 (2019).

93. Carroll, T. J., McNamee, D., Ingram, J. N. & Wolpert, D. M. Rapid visuomotor responses reflect value-based decisions. *J. Neurosci.* **39**, 3906–3920 (2019).

94. De Comite, A., Crevecoeur, F. & Lefèvre, P. Reward-Dependent Selection of Feedback Gains Impacts Rapid Motor Decisions. *Eneuro* **9**, ENEURO.0439-21.2022 (2022).

95. Codol, O. *et al.* Sensorimotor feedback loops are selectively sensitive to reward. *Elife* **12**, 1–25 (2023).

96. Krakauer, J. W., Hadjiosif, A. M., Xu, J., Wong, A. L. & Haith, A. M. Motor Learning. *Compr. Physiol.* **9**, 613–663 (2019).

97. Quattrocchi, G. *et al.* Pharmacological Dopamine Manipulation Does Not Alter Reward-Based Improvements in Memory Retention during a Visuomotor Adaptation Task. *Eneuro* **5**, ENEURO.0453-17.2018 (2018).

98. Johnson, L. *et al.* Dose-dependent effects of transcranial alternating current stimulation on spike timing in awake nonhuman primates. *Sci. Adv.* **6**, 1–9 (2020).

99. Beliaeva, V., Savvateev, I., Zerbi, V. & Polania, R. Toward integrative approaches to study the causal role of neural oscillations via transcranial electrical stimulation. *Nat. Commun.* **12**, 1–12 (2021).

100. Averbeck, B. & O'Doherty, J. P. Reinforcement-learning in fronto-striatal circuits. *Neuropsychopharmacology* **47**, 147–162 (2022).

101. Ma, I. *et al.* Ventral striatal hyperconnectivity during rewarded interference control in adolescents with ADHD. *Cortex* **82**, 225–236 (2016).

102. Wang, Q. *et al.* Dissociated neural substrates underlying impulsive choice and impulsive action. *Neuroimage* **134**, 540–549 (2016).

103. Mosley, P. E. *et al.* The structural connectivity of discrete networks underlies impulsivity and gambling in Parkinson's disease. *Brain* **142**, 3917–3935 (2019).

104. Hampton, W. H., Alm, K. H., Venkatraman, V., Nugiel, T. & Olson, I. R. Dissociable frontostriatal white matter connectivity underlies reward and motor impulsivity. *Neuroimage* **150**, 336–343 (2017).

105. Negahbani, E., Kasten, F. H., Herrmann, C. S. & Fröhlich, F. Targeting alpha-band oscillations in a cortical model with amplitude-modulated high-frequency transcranial electric stimulation. *Neuroimage* **173**, 3–12 (2018).

106. Cohen, J. *Statistical power analysis for the behavioral sciences*. *L. Erlbaum Associates* **13**, (1988).

107. Hashemirad, F., Zoghi, M., Fitzgerald, P. B. & Jaberzadeh, S. The effect of anodal transcranial direct current stimulation on motor sequence learning in healthy individuals: A systematic review and meta-analysis. *Brain Cogn.* **102**, 1–12 (2016).

108. Soutschek, A., Kang, P., Ruff, C. C., Hare, T. A. & Tobler, P. N. Brain Stimulation Over the Frontopolar Cortex Enhances Motivation to Exert Effort for Reward. *Biol. Psychiatry* **84**, 38–45 (2018).

109. Wischnewski, M., Zerr, P. & Schutter, D. J. L. G. Effects of Theta Transcranial Alternating Current Stimulation Over the Frontal Cortex on Reversal Learning. *Brain Stimul.* **9**, 705–711 (2016).

110. Guerra, A., López-Alonso, V., Cheeran, B. & Suppa, A. Variability in non-invasive brain stimulation studies: Reasons and results. *Neurosci. Lett.* **719**, 133330 (2020).

111. Cassarà, A. M. *et al.* Safety Recommendations for Temporal Interference Stimulation in the Brain. *bioRxiv* 1–69 (2022). doi:10.1101/2022.12.15.520077

112. Oldfield, R. C. The assessment and analysis of handedness: The Edinburgh inventory. *Neuropsychologia* **9**, 97–113 (1971).

113. Kaplan, B. A. *et al.* Automating Scoring of Delay Discounting for the 21- and 27-Item Monetary Choice Questionnaires. *Behav. Anal.* **39**, 293–304 (2016).

114. Mitchell, M. R. & Potenza, M. N. Recent Insights into the Neurobiology of Impulsivity. *Curr. Addict. Reports* **1**, 309–319 (2014).

1666   115. Brainard, D. H. The Psychophysics Toolbox. *Spat. Vis.* **10**, 433–436 (1997).

1667   116. Pelli, D. G. The VideoToolbox software for visual psychophysics: transforming

1668   numbers into movies. *Spat. Vis.* **10**, 437–442 (1997).

1669   117. Dayan, E., Averbeck, B. B., Richmond, B. J. & Cohen, L. G. Stochastic

1670   reinforcement benefits skill acquisition. *Learn. Mem.* **21**, 140–142 (2014).

1671   118. Grossman, N. Modulation without surgical intervention. *Science (80-.).* **361**, 461–

1672   462 (2018).

1673   119. Antal, A. *et al.* Low intensity transcranial electric stimulation: Safety, ethical, legal

1674   regulatory and application guidelines. *Clin. Neurophysiol.* **128**, 1774–1809 (2017).

1675   120. Ekhtiari, H. *et al.* A checklist for assessing the methodological quality of concurrent

1676   tES-fMRI studies (ContES checklist): a consensus study and statement. *Nat.*

1677   *Protoc.* **17**, 596–617 (2022).

1678   121. Bossetti, C. A., Birdno, M. J. & Grill, W. M. Analysis of the quasi-static

1679   approximation for calculating potentials generated by neural stimulation. *J. Neural*

1680   *Eng.* **5**, 44–53 (2008).

1681   122. Hasgall, P. *et al.* "IT'IS Database for thermal and electromagnetic parameters of

1682   biological tissues," Version 4.1. (2022). doi:10.13099/VIP21000-04-1

1683   123. Seeck, M. *et al.* The standardized EEG electrode array of the IFCN. *Clin.*

1684   *Neurophysiol.* **128**, 2070–2077 (2017).

1685   124. Bates, D., Mächler, M., Bolker, B. M. & Walker, S. C. Fitting linear mixed-effects

1686   models using lme4. *J. Stat. Softw.* **67**, (2015).

1687   125. Ryu, E. Effects of skewness and kurtosis on normal-theory based maximum

1688   likelihood test statistic in multilevel structural equation modeling. *Behav. Res.*

1689   *Methods* **43**, 1066–1074 (2011).

1690   126. Nieuwenhuis, R., te Grotenhuis, M. & Pelzer, B. Influence.ME: Tools for detecting

1691   influential data in mixed effects models. *R J.* **4**, 38–47 (2012).

1692   127. Luke, S. G. Evaluating significance in linear mixed-effects models in R. *Behav.*

1693   *Res. Methods* **49**, 1494–1502 (2017).

1694   128. Searle, S. R., Speed, F. M. & Milliken, G. A. Population marginal means in the

1695   linear model: An alternative to least squares means. *Am. Stat.* **34**, 216–221

1696   (1980).

1697   129. Ben-Shachar, M., Lüdecke, D. & Makowski, D. effectsize: Estimation of Effect Size

1698   Indices and Standardized Parameters. *J. Open Source Softw.* **5**, 2815 (2020).

1699   130. Derosière, G., Billot, M., Ward, E. T. & Perrey, S. Adaptations of motor neural

1700   structures' activity to lapses in attention. *Cereb. Cortex* **25**, 66–74 (2015).

1701   131. Okamoto, M. *et al.* Three-dimensional probabilistic anatomical cranio-cerebral

1702   correlation via the international 10-20 system oriented for transcranial functional

1703   brain mapping. *Neuroimage* **21**, 99–111 (2004).

1704   132. Di, X., Zhang, Z. & Biswal, B. B. Understanding psychophysiological interaction

1705   and its relations to beta series correlation. *Brain Imaging Behav.* **15**, 958–973

1706   (2021).

1707   133. Bowles, S. *et al.* Vagus nerve stimulation drives selective circuit modulation

1708   through cholinergic reinforcement. *Neuron* **110**, 2867-2885.e7 (2022).

1709   134. Codol, O., Galea, J. M., Jalali, R. & Holland, P. J. Reward-driven enhancements in

1710   motor control are robust to TMS manipulation. *bioRxiv* 2020.01.12.903419 (2020).

1711   doi:10.1101/2020.01.12.903419

1712   135. Draganski, B. *et al.* Evidence for segregated and integrative connectivity patterns

1713   in the human basal ganglia. *J. Neurosci.* **28**, 7143–7152 (2008).

1714   136. Morris, L. S. *et al.* Fronto-striatal organization: Defining functional and

1715   microstructural substrates of behavioural flexibility. *Cortex* **74**, 118–133 (2016).

1716   137. Lam, S. Y. & Zénon, A. Information rate in humans during visuomotor tracking.

1717   *Entropy* **23**, 1–13 (2021).

1718   138. Uehara, S., Mawase, F., Therrien, A. S., Cherry-Allen, K. M. & Celnik, P.

1719   Interactions between motor exploration and reinforcement learning. *J.*

1720   *Neurophysiol.* **122**, 797–808 (2019).

1721   139. Rolls, E. T., Huang, C. C., Lin, C. P., Feng, J. & Joliot, M. Automated anatomical

1722   labelling atlas 3. *Neuroimage* **206**, 116189 (2020).

1723